

Portland State University

**PDXScholar**

---

Biology Faculty Publications and Presentations

Biology

---

10-20-2022

# Enriched Dietary Saturated Fatty Acids Induce Trained Immunity via Ceramide Production that Enhances Severity of Endotoxemia and clearance of infection

Amy L. Seufert

*Portland State University*

James W. Hickman

*Portland State University*

Ste K. Traxler

*Portland State University*

Rachael M. Peterson

*Portland State University*

Sydney L. Lashley

*VA Portland Health Care System, Portland*

Follow this and additional works at: [https://pdxscholar.library.pdx.edu/bio\\_fac](https://pdxscholar.library.pdx.edu/bio_fac)



Part of the [Biology Commons](#)

*See next page for additional authors*

**Let us know how access to this document benefits you.**

---

## Citation Details

Seufert, A. L., Hickman, J. W., Traxler, S. K., Peterson, R. M., Waugh, T. A., Lashley, S. J., ... & Napier, B. A. (2022). Enriched dietary saturated fatty acids induce trained immunity via ceramide production that enhances severity of endotoxemia and clearance of infection. *Elife*, 11, e76744.

This Article is brought to you for free and open access. It has been accepted for inclusion in Biology Faculty Publications and Presentations by an authorized administrator of PDXScholar. Please contact us if we can make this document more accessible: [pdxscholar@pdx.edu](mailto:pdxscholar@pdx.edu).

---

**Authors**

Amy L. Seufert, James W. Hickman, Ste K. Traxler, Rachael M. Peterson, Sydney L. Lashley, Natalia Shulzhenko, Ruth J. Napier, Brooke A. Napier, and multiple additional authors

**Enriched dietary saturated fatty acids induce trained immunity via ceramide production that enhances severity of endotoxemia and clearance of infection**

Seufert AL<sup>1</sup>, Hickman JW<sup>1</sup>, Traxler SK<sup>1</sup>, Peterson RM<sup>1</sup>, Waugh TA<sup>1</sup>, Lashley SJ<sup>2</sup>, Shulzhenko N<sup>3</sup>, Napier RJ<sup>2,4</sup>,  
and Napier BA<sup>1,\*</sup>

Author Affiliations: <sup>1</sup>Department of Biology and Center for Life in Extreme Environments, Portland State University, Portland, OR, 97201, <sup>2</sup>VA Portland Health Care System, Portland, OR, 97239, <sup>3</sup>Department of Biomedical Sciences, Oregon State University, Corvallis, OR, <sup>4</sup>Department of Molecular Microbiology and Immunology, Oregon Health & Science University, Portland, OR, 97239, United States.

\*Corresponding Author: Dr. Brooke A Napier

Robertson Life Sciences Building

6<sup>th</sup> Floor Rm 6N087

Portland, OR 97201

E-mail address: brnapier@pdx.edu

## 29 **Abstract**

30 Trained immunity is an innate immune memory response that is induced by primary microbial or sterile stimuli  
31 that sensitizes monocytes and macrophages to a secondary pathogenic challenge, reprogramming the host  
32 response to infection and inflammatory disease. Nutritional components, such as dietary fatty acids, can act as  
33 inflammatory stimuli, but it is unknown if they can act as the primary stimuli in the context of innate immune  
34 memory. Here we find mice fed a diet enriched exclusively in saturated fatty acids (SFAs; ketogenic diet; KD)  
35 confer a hyper-inflammatory response to systemic lipopolysaccharide (LPS) and increased mortality,  
36 independent of diet-induced microbiome and glycemic modulation. We find KD mediates the composition of the  
37 hematopoietic stem cell (HSC) compartment, and macrophages derived from the bone marrow of mice fed KD  
38 do not have altered baseline inflammation, but enhanced responses to a secondary inflammatory challenge.  
39 Lipidomics identified enhanced free palmitic acid (PA) and PA-associated lipids in KD-fed mice serum. We  
40 found pre-treatment with physiologically relevant concentrations of PA alone reprograms macrophages to  
41 induce a hyper-inflammatory response to secondary challenge with LPS. This response was found to be  
42 dependent on the synthesis of ceramide, and reversible when treated with a ceramide synthase inhibitor. *In*  
43 *vivo*, we found systemic PA confers enhanced inflammation and mortality during an acute inflammatory  
44 response to systemic LPS, and this phenotype was not reversible for up to 7 days post-PA-exposure. While  
45 PA-treatment is harmful for endotoxemia outcome, we find PA exposure enhanced clearance of *Candida*  
46 *albicans* in *Rag1<sup>-/-</sup>* mice. Further, we show that oleic acid (OA), a mono-unsaturated FA that depletes  
47 intracellular ceramide, reverses the PA-induced hyper-inflammatory response shown in macrophages treated  
48 with LPS, and reduces severity and mortality of LPS endotoxin stimulation, highlighting the plasticity of SFA-  
49 dependent enhanced endotoxemia severity *in vivo*. These are the first data to implicate enriched dietary SFAs,  
50 and specifically PA, in the induction of long-lived innate immune memory that is detrimental during an acute  
51 inflammatory response, but beneficial for clearance of pathogens.

## 52 53 **Introduction**

54 Historically, immune memory has been defined as a trait limited to the adaptive immune system, however it is  
55 now well established that innate immune cells have the capacity for metabolic, epigenetic, and functional  
56 reprogramming that leads to long-lasting increases in host resistance to infection (1-4). Specifically, trained

immunity is an adaptation of innate host defense in vertebrates and invertebrates that results from exposure to a primary inflammatory stimulus and leads to a faster and greater response to a secondary challenge. Unlike adaptive memory responses, trained immunity does not require genome rearrangements, B and T lymphocytes, and receptors that recognize specific antigens (1-4). Further, trained immunity has been documented in organisms that lack canonical adaptive immune responses, such as plants and invertebrates, suggesting this is a primitive immune memory system that is conserved throughout vertebrates and invertebrates (5).

The Bacillus Calmette-Guérin (BCG) vaccine and yeast  $\beta$ -glucans are canonical inducers of trained immunity in humans and stimulate long-lasting metabolic and epigenetic reprogramming of myeloid-lineage cells resulting in hyperresponsiveness upon restimulation with heterologous or homologous inflammatory stimuli. This innate immune memory has been shown to be heritable (6) and can last up to months in humans and mice (7) and, thus, likely evolved to provide non-specific protection from secondary infections. Most recently, it was described that countries with higher rates of BCG vaccine at birth had fewer coronavirus disease 2019 (COVID-19) cases (8) making this immunological phenomenon extremely relevant. Importantly, it is easily ascertained that inflammatory hyperresponsiveness could be deleterious in the context of diseases where more inflammation can lead to greater pathology (ex: acute septic shock, autoimmune disorders, and allergies). Thus, trained immunity can be regarded as a double-edged sword – providing increased resistance to tissue-specific infection but exacerbating diseases exacerbated by systemic inflammation. Consequently, identifying novel inducers of trained immunity will provide clinically relevant insight into harnessing innate immune cells to attain long-term therapeutic benefits in a range of infections and inflammatory diseases.

Typically, the primary inflammatory stimulus that initiates trained immunity are danger- or pathogen-associated molecular patterns (DAMPs; PAMPs); however, recent publications have shown that  $\beta$ -glucan found in mushrooms, baker's and brewer's yeast, wheat and oats, and unknown components of bovine milk can induce trained innate immune memory in monocytes *in vitro* (9, 10). Our data reported here contribute to the growing evidence supporting the multifaceted immunoregulatory role of certain dietary constituents.

Currently, Westernized nations are increasingly dependent on diets enriched in saturated fatty acids (SFAs) (11-13), which have been shown to mimic PAMP effects on inflammatory cells, regulate innate immune cell function and alter outcomes of inflammatory disease and infection (14-17). Specifically, we have shown the

85 Western diet (WD), a diet enriched in sucrose and SFAs, correlates with increased disease severity and  
86 mortality in response to systemic LPS, independent of the diet-dependent microbiota, demonstrating the  
87 possibility that the dietary components of this diet may be driving the hyperresponsiveness to LPS (18).  
88 Currently, it is unknown if enriched dietary SFAs alone mediate trained immunity.

89 Our work presented herein identifies a ketogenic diet (KD) enriched exclusively in SFAs, and not  
90 sucrose, confers an increased systemic response to LPS independent of diet-associated microbiome, ketosis,  
91 or glycolytic regulation during disease, and alters inflammatory capacity and composition of the hematopoietic  
92 compartment. While others have shown that the WD induces trained immunity in atherosclerotic mice (*Ldlr*<sup>-/-</sup>),  
93 we are the first to show that trained immunity, including its hallmark long-term persistence, can be induced in  
94 wild-type (WT) mice with exposure to enriched SFAs alone (19). A lipidomic analysis of blood fat composition  
95 after KD exposure revealed a significant increase of free palmitic acid (PA; C16:0) and fatty acid complexes  
96 containing PA. PA is known to act synergistically with LPS to enhance intracellular ceramide levels and  
97 proinflammatory cytokine expression in macrophages, however it is currently unknown if ceramide, a bioactive  
98 sphingolipid, specifically mediates a heightened inflammatory response to LPS following pre-exposure to PA  
99 (20, 21). Here we find macrophages pre-treated with physiologically relevant concentrations of PA followed by  
100 a secondary exposure to LPS leads to enhanced proinflammatory cytokine expression and release, which was  
101 reversible with the inhibition of ceramide.

102 We find that both short- and long-term exposure to PA, the predominant SFA found in high-fat diets,  
103 enhances systemic response to microbial ligands in mice even after a 7-day rest period from PA exposure.  
104 Thus, our data suggest exposure to PA leads to a long-lasting innate immune memory response *in vivo* (7).  
105 Importantly, trained immunity is induced when a primary inflammatory stimulus changes transcription of  
106 inflammatory genes, the immune status returns to basal levels, and challenge with a secondary stimulus  
107 enhances transcription of inflammatory cytokines at much higher levels than those observed during the primary  
108 challenge (22). While the dynamics of an initial inflammatory event induced by PA *in vivo* are not defined in this  
109 paper, we show that basal levels of *Tnf*, *Il6*, *Il1b* and *Il10* in the blood of mice pre-exposed to PA were  
110 comparable to control mice immediately prior to endotoxin challenge, indicating that mice were not in a primed  
111 state prior to disease. This suggests that the hyper-inflammation and poor disease outcome we show in PA-  
112 exposed mice is not due to priming, but a trained immune response.

113 The dual nature of trained immunity is also a hallmark feature of the phenomenon, in that non-specific  
114 innate immune memory can be either beneficial or detrimental depending on the disease context. The majority  
115 of research has demonstrated the protective role of trained immunity against a variety of infections, such as  
116 with BCG vaccination and B-glucan stimulation (3, 23). Our work is unique because we focus on the  
117 detrimental role that trained immunity has on disease characterized by inflammatory dysregulation, however  
118 we also highlight the beneficial nature of this novel phenotype by showing that when mice lacking adaptive  
119 immunity (*Rag1<sup>-/-</sup>*) are pre-exposed to systemic PA, they exhibit enhanced clearance of kidney fungal burden  
120 compared to control mice.

121 We further identify a novel role of SFA-dependent intracellular ceramide required for the enhanced  
122 systemic response to microbial ligands, and show intervention with oleic acid, a mono-unsaturated fatty acid  
123 that depletes PA-dependent ceramide, can reverse these phenotypes in macrophages and *in vivo*. Our data  
124 presented here highlight the dynamic plasticity of dietary intervention on inflammatory disease outcomes.  
125 These data are consistent with the current knowledge that SFAs and ceramide are immunomodulatory  
126 molecules, and build on these by highlighting a previously unidentified role of PA in driving long-lived trained  
127 immunity.

## 129 **Results**

### 130 **Diets enriched in saturated fatty acids increase endotoxemia severity and mortality**

131 To examine the immune effects of chronic exposure to diets enriched in SFAs on lipopolysaccharide (LPS)-  
132 induced endotoxemia, we fed age matched (6 – 8 wk), female BALB/c mice either a WD (enriched in SFAs and  
133 sucrose), a ketogenic diet (KD; enriched in SFAs and low-carbohydrate), or standard chow (SC; low in SFAs  
134 and sucrose), for 2 weeks (wk) (Supplementary File 1). We defined 2 wk of feeding as chronic exposure,  
135 because this is correlated with WD- or KD-dependent microbiome changes, and confers metaflammation in  
136 WD mice (18), sustained altered blood glucose levels in WD mice (Fig 1 - figure supplement 1A), and elevated  
137 levels of ketones in the urine and blood in KD mice (Fig 1 - figure supplement 1 B-C). We then induced  
138 endotoxemia by a single intraperitoneal (i.p.) injection of LPS. We measured hypothermia as a measure of  
139 disease severity and survival to determine outcome (18, 24, 25). WD- and KD-fed mice showed significant and  
140 prolonged hypothermia, starting at 10 hours (h) post-injection (p.i.), compared to the SC-fed mice (Fig 1A). In

141 accordance with these findings, WD- and KD-fed mice displayed 100% mortality by 26 h p.i. compared to  
142 100% survival of SC-fed mice (Fig 1B). Hypoglycemia is a known driver of endotoxemia, and each of these  
143 diets has varying levels of sugars and carbohydrates (Supplementary File 1) (26, 27). However, mice in all diet  
144 groups displayed similar levels of LPS-induced hypoglycemia during disease (Fig 1 - figure supplement 1D),  
145 indicating that potential effects of diet on blood glucose were not a driver of enhanced disease severity.

146 Considering mice fed KD experience a shift towards nutritional ketosis, we wanted to understand if our  
147 phenotype was dependent on nutritional ketosis. 1,3-butanediol is a compound that induces ketosis by  
148 enhancing levels of the ketone  $\beta$ -hydroxybutyrate in the blood (28). Age matched (6 – 8 wk), female BALB/c  
149 mice were fed for 2 wk with KD, SC supplemented with saccharine and 1,3-butanediol (SC + BD) or SC-fed  
150 with the saccharine vehicle solution (SC + Veh). BD supplementation was sufficient to increase blood ketones  
151 (Fig 1 - figure supplement 1 C). We next injected LPS i.p. and found KD-fed mice showed significantly greater  
152 hypothermia, and increased mortality, compared to SC + BD and SC + Veh (Fig 1 - figure supplement 1 E-F).  
153 Though short-lived, when compared to SC + Veh, the SC + BD mice did confer an increase in hypothermia,  
154 suggesting that nutritional ketosis may play a minor role in KD-dependent susceptibility to endotoxemia (Fig 1 -  
155 figure supplement 1 E-F). Together these data suggest that diets enriched in SFAs promote enhanced acute  
156 endotoxemia severity and this is independent of diet-dependent hypoglycemic shock or nutritional ketosis.

### 157 **Diets enriched in SFAs induce a hyper-inflammatory response to LPS and increased immunoparalysis**

158 Endotoxemia mortality results exclusively from a systemic inflammatory response characterized by an acute  
159 increase in circulating inflammatory cytokine levels (ex: TNF, IL-6, and IL-1 $\beta$ ) from splenocytes and myeloid  
160 derived innate immune cells (29-32). Additionally, pre-treatment of myeloid-derived cells with dietary SFAs has  
161 been shown to enhance inflammatory pathways in response to microbial ligands (33, 34). Considering this, we  
162 hypothesized that exposure to enriched systemic dietary SFAs in WD- and KD-fed mice would enhance the  
163 inflammatory response to systemic LPS during the acute inflammatory response. Five-hours p.i., age matched  
164 (6 – 8 wk), female BALB/c mice fed all diets showed induction of *Tnf*, *Il6*, and *Il1b* expression in the blood (Fig  
165 1C-E). However, at 5 h p.i., WD- and KD-fed mice experienced significantly higher expression of *Tnf* and *Il6* in  
166 the blood, compared with SC-fed mice, and WD-fed mice also showed significantly higher *Il1b* expression (Fig  
167 1C-E), indicating that diets enriched in SFAs are associated with a hyper-inflammatory response to LPS.  
168



169 Importantly, septic patients often present with two immune phases: an initial amplification of  
170 inflammation, followed-by or concurrent-with an induction of immune suppression (immunoparalysis), that can  
171 be measured by a systemic increase in the anti-inflammatory cytokine IL-10 (35, 36). Further, in septic  
172 patients, a high IL-10:TNF ratio equates with the clinical immunoparalytic phase and correlates with poorer  
173 sepsis outcomes (37, 38). Interestingly, we found there was significantly increased *Il10* expression in WD- and  
174 KD-fed mice, compared to SC-fed mice (Fig 1F), and WD- and KD-fed mice had significantly higher *Il10:Tnf*  
175 ratios at 10-20 h and 15-20 h, respectively, compared to SC-fed mice (Fig 1G). These data conclude that mice  
176 exposed to diets enriched in SFAs show an initial hyper-inflammatory response to LPS, followed by an  
177 increased immunoparalytic phenotype, which correlates with enhanced disease severity, similar to what is  
178 seen in the clinic.

#### 180 **Diets enriched in SFAs drive enhanced responses to systemic LPS independent of diet-associated** 181 **microbiome**

182 We have previously shown that WD-fed mice experience increased endotoxemia severity and mortality,  
183 independent of diet-associated microbiome (18). In order to confirm the increases in disease severity that  
184 correlated with KD were also independent of KD-associated microbiome changes, we used a germ free (GF)  
185 mouse model. 19-23 wk old female and 14 – 23 wk old male and female GF C57BL/6 mice were fed SC, WD,  
186 and KD for 2 wk followed by injection with 50 mg/kg of LPS, our previously established LD<sub>50</sub> in GF C57BL/6  
187 mice (18). As we saw in the conventional mice, at 10 h p.i. WD- and KD-fed GF mice showed enhanced  
188 hypothermia and mortality, compared to SC-fed GF mice (Fig 1H, I). These data show that, similar to WD-fed  
189 mice, the KD-associated increase in endotoxemia severity and mortality is independent of diet-associated  
190 microbiome.

191 Our previous studies (Fig 1A-G) in conventional mice were carried out in 6 – 8 wk female mice on a  
192 BALB/c background. Importantly, genetic background and age differences can have large effects on LPS  
193 treatment outcome. The GF mice used in this study (Fig 1H-N) were on a C57BL/6 background, between the  
194 ages of 14 – 23 wk. Thus, we confirmed WD- and KD-fed conventional C57BL/6 mice aged 20 – 21 wk old  
195 show enhanced disease severity and mortality in an LPS-induced endotoxemia model (4.5 mg/kg), compared  
196 to mice fed SC, similar to what is seen in younger BALB/c mice (Fig 1 - figure supplement 1 G-H).

197 Additionally, to confirm that the hyper-inflammatory response to systemic LPS was independent of the  
198 WD- and KD-dependent microbiome, we measured systemic inflammation during endotoxemia via the  
199 expression of *Tnf*, *Il6*, and *Il1b* in the blood at 0-10 h p.i. We found, WD- and KD-fed GF mice displayed  
200 enhanced expression of *Tnf* and *Il1b* at 5-10 h, and significantly enhanced expression of *il-6* at 5 h, compared  
201 to SC-fed GF mice (Fig 1J-L). Interestingly, *Il10* expression and the *Il10:Tnf* ratio were not significantly different  
202 throughout all diets, suggesting the SFA-dependent enhanced immunoparalytic phenotype is dependent on the  
203 diet-associated microbiomes in WD- and KD-fed mice (Fig 1M-N). These data demonstrate that the early  
204 hyper-inflammatory response, but not the late immunoparalytic response, to LPS associated with enriched  
205 dietary SFAs is independent of the diet-dependent microbiota.

### 207 **A diet enriched exclusively in SFAs induces trained immunity**

208 Thus far we find feeding diets enriched in SFAs (WD and KD) leads to enhanced expression of inflammatory  
209 cytokines in the blood after treatment with systemic LPS, suggesting that the SFAs may be inducing an innate  
210 immune memory response that leads to a hyper-inflammatory response to secondary challenge. Specifically,  
211 trained immunity is an innate immune memory response characterized by reprogramming of myeloid cells by a  
212 primary inflammatory stimulus, that then respond more robustly to secondary inflammatory challenge. Trained  
213 immunity has been shown to mediate cell sub-types within the hematopoietic stem cell (HSC) compartment  
214 that give rise to “trained” myeloid progeny for weeks to years (39). A previous study in *Ldlr<sup>-/-</sup>* mice has shown 4  
215 wk of WD feeding significantly enhances multipotent progenitors (MPPs) and granulocyte and monocyte  
216 precursors (GMPs) and skews development of GMPs toward a monocyte lineage that are primed to respond  
217 with a hyper-inflammatory response to LPS (19). Currently, it is unknown if diets enriched in SFAs fed to WT  
218 mice, can induce changes within the HSC compartment or long-lasting trained immunity.

219 In order to determine the impact of dietary SFAs on bone marrow reprogramming *in vivo*, we next  
220 evaluated HSCs and progenitor cells via FACS from age-matched (6 – 8 wk) female WT BALB/c mice fed SC,  
221 WD and KD for 2 wk. Using previously published panels for analyzing HSC populations in the bone marrow  
222 (23, 40, 41), we collected bone marrow and measured relative proportions of long-term HSCs (LT-HSCs;  
223 CD201<sup>+</sup>CD27<sup>+</sup>CD150<sup>+</sup>CD48<sup>-</sup>), short-term HSCs (ST-HSCs; CD201<sup>+</sup>CD27<sup>+</sup>CD150<sup>+</sup>CD48<sup>+</sup>), and multipotent  
224 progenitors (MPPs; CD201<sup>+</sup>CD27<sup>+</sup>CD150<sup>-</sup>CD48<sup>+</sup>) (Fig 2A, B). Strikingly, we find that KD-fed mice showed

225 significantly enhanced ST- and LT-HSCs, and MPPs compared to SC-fed mice (Fig 2C). Unlike previously  
226 reported in *Ldlr*<sup>-/-</sup> mice, there was no significant change in ST-HSCs, LT-HSCs, or MPPs within WD-fed WT  
227 mice (Fig 2C). Further, we did not see a significant increase in MPP3s for WD-fed mice, as previously  
228 published for *Ldlr*<sup>-/-</sup> mice (19), or KD-fed mice; however, this may be due to the difference in genetic  
229 backgrounds, or length of diet administration (Fig 2 - figure supplement 1 A). These data are the first to show  
230 that the KD, a diet solely enriched in SFAs, alters hematopoiesis by enhancing expansion and differentiation of  
231 HSCs, similar to previously described inducers of trained immunity.

232 Further, it is unknown if enriched dietary SFAs lead to long-lasting functional reprogramming associated  
233 with trained immunity, that leads to a hyper-inflammatory response. Thus, we fed age-matched (6 – 8 wk)  
234 female BALB/c mice SC, WD, or KD for 2 wk, isolated bone marrow, differentiated into BMDMs for 7 days, and  
235 analyzed baseline inflammation and response to LPS. We found that untreated BMDMs isolated from mice fed  
236 SC and WD showed no significant differences in TNF or IL-6, and those from KD-fed mice showed a modest  
237 increase only in IL-6 compared to BMDMs from SC-fed mice (Fig 2 - figure supplement 1B). However, when  
238 BMDMs were stimulated with LPS for 24 h *ex vivo*, BMDMs from WD- and KD-fed mice showed significantly  
239 higher secretion of TNF, and only those from KD-fed mice showed significantly enhanced IL-6 secretion (Fig  
240 2D-E). These data show that diets enriched in SFAs are inducing long-lasting inflammatory reprogramming of  
241 myeloid cells *in vivo*, and that reprogramming takes place within the bone marrow.

242 Importantly, monocytes and splenocytes are necessary for induction of systemic inflammatory  
243 cytokines during endotoxemia (31, 32). Thus, we wanted to assess if enriched dietary SFA induces *in vivo*  
244 reprogramming of monocytes and splenocytes, leading to an enhanced response to LPS *ex vivo*. First, we fed  
245 age-matched (6 – 8 wk) female BALB/c mice SC, WD, or KD for 2 wk, isolated bone marrow monocytes  
246 (BMMs) via magnetic negative selection using bone marrow extracted from femurs and tibias, and determined  
247 baseline expression of inflammatory cytokines. We found that prior to *ex vivo* LPS stimulation, BMMs isolated  
248 from mice fed SC, WD, or KD showed no significant difference in *Tnf* expression, and *Il6* expression was  
249 significantly decreased in BMMs from KD-fed mice (Fig 2 - figure supplement 1 C). However, when BMMs  
250 were stimulated with LPS for 2 h *ex vivo*, those from KD-fed mice showed significantly higher expression of *Tnf*  
251 and *Il6*, while those from WD-fed mice exhibited no significance in expression compared to SC-fed mice (Fig 2  
252 - figure supplement 1 D). Similarly, we isolated splenocytes from SC-, WD-, and KD-fed mice and found no

253 difference between homeostatic inflammation of splenocytes between diets, but a significantly enhanced  
254 expression of *Tnf* in the splenocytes of KD-fed mice, and not WD-fed mice, challenged with LPS (2 h)  
255 compared to splenocytes from SC-fed mice (Fig 2 - figure supplement 1 E-F).

256 These data show the KD stimulates expansion of HSC populations, and skew differentiation of myeloid  
257 progenitors that then give rise to macrophages with enhanced inflammatory potency (Fig 2A-E; Fig 2 - figure  
258 supplement 2). Further, these data suggest that BMDMs, BMMs, and splenocytes from WD- and KD-fed mice  
259 are not more inflammatory at homeostasis; however, when challenged with LPS, KD feeding confers a hyper-  
260 inflammatory response. Together, our results suggest the KD, a diet that is comprised of 90.5% SFAs, leads to  
261 reprogramming of the HSC compartment and long-lasting trained immunity.

### 263 **Palmitic acid (PA) and PA-associated fatty acids are enriched in the blood of KD-fed mice**

264 It is known that the SFAs consumed in the diet determine the SFA profiles in the blood (42-44) and that these  
265 SFAs have the potential to be immunomodulatory. Thus, we next wanted to identify target SFAs enriched in  
266 the blood of mice fed a diet exclusively enriched in SFAs that may be altering the systemic inflammatory  
267 response to LPS. Considering that the KD is enriched in SFAs and not sucrose, and that KD-fed mice showed  
268 distinct HSC alterations and LPS-induced hyper-inflammation in BMDMs, BMMs, and splenocytes treated *ex*  
269 *vivo*, the subsequent studies were performed exclusively on KD-fed mice. We used mass spectrometry  
270 lipidomics to create diet-dependent profiles of circulating fatty acids in SC- and KD-fed mice (45). Age matched  
271 (6 – 8 wk), female BALB/c mice were fed SC or KD for 2 wk, then serum samples were collected and analyzed  
272 using qualitative tandem liquid chromatography quadrupole time of flight mass spectrometry (LC-QToF  
273 MS/MS). We used principal component analysis (PCA) to visualize how samples within each data set clustered  
274 together according to diet, and how those clusters varied relative to one another in abundance levels of free  
275 fatty acids (FFA), triacylglycerols (TAG), and phosphatidylcholines (PC). For all three groups of FAs, individual  
276 mice grouped with members of the same diet represented by a 95% confidence ellipse with no overlap  
277 between SC- and KD-fed groups (Fig 3A-C). These data indicate that 2 wk of KD feeding is sufficient to alter  
278 circulating FFAs, TAGs, and PCs, and that SC- and KD-fed mice display unique lipid blood profiles. Similarly,  
279 the relative abundance of sphingolipids (SG) in SC- and KD-fed mice displayed unique diet-dependent profiles  
280 with no overlapping clusters, and abundance of specific SGs were significantly higher in the serum of KD-fed

281 mice compared to SC-fed mice (Fig 3 - figure supplement 1 A-B). Though the independent role of each FFA,  
282 TAG, PC, and SG species has not been clinically defined, each are classes of lipids that when accumulated is  
283 associated with metabolic diseases, which have been shown to enhance susceptibility to sepsis and  
284 exacerbate inflammatory disease (16, 46-48).

285 Importantly, we identified a significant increase in multiple circulating FFAs within the KD-fed mice,  
286 compared to the SC-fed mice, many of which were SFAs (Fig 3D). Interestingly, in KD-fed mice we found a  
287 significant increase in free palmitic acid (PA; C16:0), an immunomodulatory SFA that is found naturally in  
288 animal fats, vegetable oils, and human breast milk (49), and is 8-fold enriched in KD (Fig 3D, Supplementary  
289 File 1). Additionally, PA-containing TAGs and PCs were significantly elevated in KD-fed mice serum, compared  
290 to SC-fed mice (Fig 3 - figure supplement 1 C-D). These data indicate that KD feeding not only enhances  
291 levels of freely circulating PA, but also enhances the frequency PA is incorporated into other lipid species in  
292 the blood.

### 293 294 **Palmitic acid enhances macrophage inflammatory response to lipopolysaccharide**

295 Many groups have shown that PA alone induces a modest, but highly reproducible increase in the expression  
296 and release of inflammatory cytokines in macrophages and monocytes (14, 50). However, it remains unknown  
297 if PA can act as a primary inflammatory stimulus to induce a hyper-inflammatory response to a secondary  
298 heterologous stimulus in primary cells. Thus, we next wanted to determine if pre-exposure to physiologically  
299 relevant concentrations of PA altered the macrophage response to a secondary challenge with LPS. Current  
300 literature indicates a wide range of serum PA levels, between 0.3 – 4.1 mM, reflect a high-fat diet in humans  
301 (51) (52-55). We aimed to use a physiologically relevant concentration of PA reflecting a human host for our *in*  
302 *vitro* studies, thus we treated primary bone marrow-derived macrophages (BMDMs) with and without 1 mM of  
303 PA containing 2% bovine serum albumin (BSA) for 12 h, removed the media, subsequently treated with LPS  
304 (10 ng/mL) for an additional 24 h, and measured expression and release of TNF, IL-6, and IL-1 $\beta$ . Importantly,  
305 the BSA dissolved in the media used for PA treatment solutions was endotoxin- and FA-free to ensure aberrant  
306 TLR signaling would not occur via BSA-contamination, and fresh PA was conjugated to BSA-containing media  
307 immediately prior to use. We found that BMDMs pre-treated with PA (1 mM) for 12 h expressed significantly  
308 higher levels of *Tnf* and *Il6* in response to secondary treatment with LPS, compared to naïve BMDMs (Fig 3E,

F). *I11b* expression was significantly lower in cells pre-treated with PA (Fig 3G), however, secretion of TNF, IL-6 and IL-1 $\beta$  were all enhanced in BMDMs pre-treated with PA (1 mM) for 12 h and challenged with LPS (Fig 3H-J). We found a similar enhanced *I16* and *Tnf* expression in response to LPS in BMDMs treated with PA (1 mM) for twice the length of exposure (24 h), and *I1-1b* expression was decreased (Fig 3 - figure supplement 2 A-C).

Further, we pre-treated BMDMs with a concentration of PA that reflects the lower range of physiologically relevant serum levels and found 0.5 mM of PA induced significantly higher expression of *Tnf*, *I16* and *I11b* after 12 h challenge with LPS, however only *Tnf* and *I16* were significantly enhanced after 24 h LPS treatment, compared to naive BMDMs treated with LPS (Fig 3 - figure supplement 2 D-I).

Importantly, PA-treatment can induce apoptosis and pyroptosis in various cell types (56-59), however we found only an average of 3.4% and 4.4% of cell death after a 12 h or 24 h incubation, respectively, with PA (1 mM) and subsequent 24 h of LPS treatment or control media (Fig 3 - figure supplement 3 A-B). These data demonstrate PA pre-treatment of macrophages induces a hyper-inflammatory response to LPS independent of cell death, suggesting PA is sensitizing macrophages to secondary inflammatory challenge.

Thus, we conclude that both 12 and 24 h pre-treatments with 0.5 mM or 1 mM of PA conjugated to 2% BSA are sufficient to induce reprogramming of macrophages and alter the response to stimulation with a heterologous ligand. Additionally, these data demonstrate that even serum concentrations of PA that are at the lower end of the spectrum for humans consuming a high-fat diet pose a risk for inflammatory dysfunction.

### **Diverting ceramide synthesis inhibits the PA-dependent hyper-inflammatory response to LPS in macrophages**

PA treatment of various cell types diverts cellular metabolism toward the synthesis of the toxic metabolic byproducts: diacylglycerols (DAGs) and ceramide (60). PA-induced ceramide synthesis has specifically been demonstrated to enhance inflammation (20, 21, 33, 61). Considering this, we wanted to determine the role of enhanced macrophage ceramide production in driving PA-induced hyper-inflammatory response to LPS. Thus, we treated BMDMs simultaneously with PA (0.5 mM) and a ceramide synthase inhibitor Fumonisin B1 (FB1; 10  $\mu$ M), for 12 h, removed the media, subsequently treated with LPS (10 ng/mL) for an additional 24 h, and measured release of TNF, IL-6, and IL-1 $\beta$ . We found that BMDMs pre-treated simultaneously with PA and FB1 for 12 h expressed significantly lower levels of TNF, IL-6, and IL-1 $\beta$  secretion in response to LPS, compared to

BMDMs pre-treated with only PA (Fig 3K-M). We conclude that ceramide synthesis induced by PA is required for the macrophage hyper-inflammatory response to secondary challenge with LPS.

### **Palmitic acid is sufficient to increase endotoxemia severity and systemic hyper-inflammation**

Considering the drastic effect of PA on macrophage response to secondary challenge with LPS, we next wanted to understand if exposure to PA alone is sufficient to induce a hyper-inflammatory response during endotoxemia *in vivo*. We answered this question using age-matched (6 – 8 wk) female BALB/c mice fed SC for 2 wk, by mimicking systemic PA levels found in serum of humans on high-fat diet via a single i.p. injection of ethyl palmitate (750 mM), and then after 12 h, challenging with LPS i.p. (62). Similar to previous publications, we find that a 750 mM i.p. injection of ethyl palmitate enhances free PA levels in the serum to 173 – 425  $\mu$ M compared to Veh-treated mice with 110 – 250  $\mu$ M (Fig 4 - figure supplement 1 A). Important to note, free PA is only transiently enhanced by systemic application, and is quickly (<1 h) taken up by peripheral tissues; thus, our detected free serum levels are most likely an underestimation of transient systemic PA (63-65).

Interestingly, after LPS challenge, PA-treated mice experienced increased disease severity as indicated by their significant decline in temperature compared to Veh mice (Fig 4A). Similar to WD- and KD-fed mice, PA-treated mice also exhibited enhanced mortality, compared to Veh mice (Fig 4B). Importantly, mice injected with PA for shorter time periods (0, 3, and 6 h) and then challenged with LPS did not exhibit increased disease severity or poor survival outcome (Fig 4 - figure supplement 1 B-C), concluding that a 12 h pre-treatment with PA is required for an increase in disease severity.

Next, we measured systemic inflammatory status during disease and found similar to KD-fed mice, the 12 h PA-pre-treated mice showed significantly enhanced expression of *Tnf* (5 h and 10 h) and *Il6* (5 h) post-LPS challenge, compared to Veh control (Fig 4C, D). Expression of *Il-1b* trended upward, but was not significantly up-regulated in 12 h PA-pre-treated mice, compared to Veh-treated mice (Fig 4E). Importantly, as a control we looked at LPS-induced hypoglycemia in PA-treated mice, and 12 h pre-treatment with PA did not alter LPS-induced hypoglycemia (Fig 4 - figure supplement 1 D), indicating that diet-dependent hypoglycemic shock was not a driver of endotoxemia severity in PA-treated mice. Thus, exposure to PA to mimic systemic levels found in humans eating high-fat diets is sufficient to drive enhanced inflammation and disease severity in mice stimulated with endotoxin, and this effect is dependent on length of PA exposure.

### PA induces long-lived hyperresponsiveness to LPS and enhanced clearance of fungal infection

Our data show that pre-treatment with systemic PA alone enhances endotoxemia severity *in vivo*, and enhances inflammatory responses of macrophages to a secondary and heterologous stimulus *in vitro*. This form of regulation resembles trained immunity; however, it remains unclear if PA is inducing trained immunity *in vivo*. We first evaluated the basal level expression of *Tnf*, *Il6*, and *Il1b* in mice treated with 750 mM of PA or Veh i.p. for 12 h, before stimulation with LPS. Interestingly, we did not see significant differences in *Tnf*, *Il6*, or *Il1b* expression at 12 h of exposure with PA (Fig 4F), which suggests that circulating immune cells of these mice are not in a primed state at these time points prior to LPS injection. These data suggest PA induces trained immunity, and not priming, however the time point of initial inflammation induced by PA remains unknown.

As mentioned previously, canonical inducers of trained immunity (e.g., BCG or  $\beta$ -glucan) induce long-lived enhanced innate immune responses to secondary inflammatory stimuli (23, 66). Thus, we hypothesized that exposure to a PA bolus would enhance disease severity and mortality in mice, and that this phenotype would persist even after mice were rested from PA injections for 1 wk. We injected age matched (6 – 8 wk), female BALB/c mice fed SC with a vehicle solution (Veh $\rightarrow$ SC) or PA (750 mM; PA $\rightarrow$ SC) i.p. once a day for 9 d and then rested the mice for 1 wk. When challenged with systemic LPS, PA $\rightarrow$ SC showed an increase in disease severity and mortality compared to Veh $\rightarrow$ SC mice (Fig 4G, H), indicating that PA alone can induce long-lived trained immunity that increases susceptibility to inflammatory disease. Importantly, the difference between Veh $\rightarrow$ SC and PA $\rightarrow$ SC survival was not significant (Fig 4H), suggesting PA is not the sole driver of the enhanced mortality we see in KD.

Lastly, the most commonly studied models for inducing trained immunity are immunization with BCG or stimulation with  $\beta$ -glucan, and they have been shown to protect mice from systemic *Candida albicans* infection via lymphocyte-independent immunological reprogramming that leads to decreased kidney fungal burden (2). Therefore, we next tested if PA treatment induces lymphocyte-independent clearance of *C. albicans* infection. For these experiments, *Rag1* knockout (*Rag1*<sup>-/-</sup>) mice were treated with a vehicle or PA solution for 12 h and subsequently infected intravenously (i.v.) with  $2 \times 10^6$  *C. albicans*. In accordance with canonical trained immunity models, mice treated with PA for 12 h showed a significant decrease in kidney fungal burden



393 compared to Veh mice, 24 h post-infection (Fig 4I). These are the first data to suggest PA enhances innate  
394 immune clearance of *C. albicans in vivo*.

### 396 **Oleic acid reverses enhanced disease severity in WD- and KD-fed mice.**

397 We have reported here that diversion of ceramide synthesis reverses the PA-dependent hyper-inflammatory  
398 response to LPS in macrophages *in vitro* (Fig. 3K-M). Interestingly, oleic acid (C18:1) is a mono-unsaturated  
399 fatty acid naturally found in animal fats and vegetable oils, and in the presence of PA, diverts lipid metabolism  
400 away from ceramide production (60, 67). Considering OA and PA are the most prevalent fatty acids found in  
401 the human diet and in human serum (60), we wanted to test if OA diversion of ceramide synthesis could  
402 reverse the PA-dependent hyper-inflammatory response to LPS in macrophages. Thus, we treated BMDMs  
403 with OA (0.2 mM), PA (0.5 mM), or OA and PA together for 12 h and then with LPS. We found that  
404 macrophages simultaneously pre-treated with PA and OA produced significantly lower levels of TNF, IL-6, and  
405 IL-1 $\beta$  following subsequent LPS exposure, compared to BMDMs pre-treated with only PA prior to LPS  
406 stimulation (Fig 5A-C). These data reveal OA-dependent depletion of intracellular ceramides neutralizes the  
407 PA-dependent hyper-inflammatory response to LPS in macrophages.

408 Considering this, we next wanted to know if i.p. injections of OA in KD-fed mice would mitigate enriched  
409 dietary SFA-associated disease severity and mortality. Thus, we fed age-matched (6 – 8 wk) female BALB/c  
410 mice SC or KD for 2 wk and injected them i.p. with 300 mM oleic acid or Veh once per day for the final 3 d of  
411 feeding. We then injected LPS i.p. and measured hypothermia and survival. Veh-injected KD-fed mice showed  
412 significant and prolonged hypothermia starting at 8 h p.i., compared to SC-fed mice (Fig 5D). In accordance  
413 with these findings, KD-fed mice displayed significantly enhanced mortality by 24 h p.i., compared to 100%  
414 survival of SC-fed mice (Fig 5E). Strikingly, for KD-fed mice injected with 300 mM OA prior to LPS treatment,  
415 there was minimal temperature loss comparable to SC-fed mice, and 100% survival (Fig 5D, E). Together,  
416 these data show systemic OA can abrogate KD-dependent hypothermia and survival defect in response to  
417 LPS in mice fed diets enriched solely in SFA, and highlight the fascinating plasticity of dietary fatty acid  
418 reprogramming of innate immune cell populations and disease dynamics.

## 420 **Discussion**

421 In this study we showed that mice fed diets enriched in SFA exhibit hyper-inflammation during endotoxemia  
422 and poorer outcomes, compared with mice fed a standard low-SFA diet, independent of the diet-associated  
423 microbiome, ketosis, and the impact of each diet on LPS-induced hypoglycemia (Fig 1; Fig 1 - figure  
424 supplement 1). Strikingly, we found that before LPS treatment, healthy mice fed a diet solely enriched in SFAs  
425 (Ketogenic diet; KD) displayed significant expansion of HSCs, including MPPs, and harbored BMDMs, BM  
426 monocytes, and splenocytes that were not inherently more inflamed, but when challenged with LPS exhibited  
427 increased production of inflammatory cytokines (Fig 2; Fig 2 - figure supplement 1, Fig 2 - figure supplement  
428 2). Since (1) we did not confer the hyper-inflammatory phenotype in BMDMs, BMMs, and splenocytes with  
429 WD, but only from KD-fed mice, and (2) the KD is only enriched in SFAs and contains no sucrose, allowing us  
430 to ask questions specifically about SFAs, we chose to focus on the KD for the remainder of the study.

431 Considering the immunogenic properties of some dietary SFAs enriched in the KD, and that excess  
432 dietary SFAs are found circulating throughout the blood and peripheral tissues, we used lipidomics to identify  
433 dietary SFAs that may be directly reprogramming innate immune cells to respond more intensely to secondary  
434 inflammatory stimuli. Our study identified enriched palmitic acid (C16:0; PA) and PA-associated fatty acids in  
435 the blood of KD-fed mice (Fig 3; Fig 3 - figure supplement 1). And, when we treated macrophages with  
436 physiologically relevant concentrations of PA, we found that PA alone induces a hyper-inflammatory response  
437 to secondary challenge with LPS (Fig 3; Fig 3 - figure supplement 2). This enhanced production of  
438 inflammatory cytokines in response to secondary heterologous stimuli has been shown in previous models of  
439 innate immune memory, specifically trained immunity (4, 19, 68). Further, our data suggests PA induces  
440 trained immunity by showing that circulating inflammatory levels in PA-injected mice were not upregulated or in  
441 a primed state prior to LPS stimulation *in vivo* (Fig 4F), and PA-associated enhanced endotoxemia severity  
442 and mortality is still shown in mice rested for 7 days post-PA exposure (Fig 4G-H). Importantly, we have not  
443 fully defined the initial inflammatory response to PA in our model, thus our data only suggests trained immunity  
444 is induced by PA exposure. However, we do find that PA- exacerbates the acute phase of endotoxin challenge  
445 and correlates with increased mortality, but also enhances resistance to infection independent of mature  
446 lymphocytes (Fig 4). Together, our data concludes PA exposure can lead to hallmark phenotypes associated  
447 with canonical trained immunity models *in vitro* and *in vivo*.

448 Interestingly, the *in vivo* blood expression of cytokines for KD-fed mice following endotoxin challenge is  
449 mild in comparison to the cytokine secretion we show for BM monocytes, splenocytes, and BMDMs isolated  
450 from KD-fed mice treated with LPS *ex vivo* (Fig 1; Fig 2; Fig S2). The media used for culturing and treating BM  
451 monocytes and splenocytes *ex vivo* with LPS contained a high-glucose concentration (4.5 g/L; 25 mM).  
452 However, high-glucose media does not alter TNF, IL-6, or IL-1 $\beta$  secretion, or mitochondrial metabolic activity,  
453 in WT BMDMs treated with LPS following 7 d of differentiation in high-glucose media (69). Additionally, in these  
454 studies, metabolic adaptation likely takes place within 48 h for BMDMs cultured in high glucose media (69);  
455 thus, we suggest it is unlikely that high-glucose contributed to the significant augmentation of LPS-induced  
456 TNF and IL-6 secretion for BMDMs from KD-fed mice compared to controls, following 7 d of differentiation in  
457 high-glucose media prior to LPS challenge. However, further studies on the metabolic flexibility of the SC- and  
458 KD-BMDMs will be required to answer this question directly.

459 Additionally, we have previously shown that WD-induced weight gain does not correlate with enhanced  
460 endotoxemia severity and mortality in conventional mice (18). This is important to address because of the  
461 “obesity paradox” that describes the diversity in sepsis severity and mortality exhibited within the obese patient  
462 population, with some studies showing that obesity may even be protective in certain disease contexts (70).  
463 Humans on an animal-based KD that contains 76% fat with 30% SFA content, and 10% carbohydrates,  
464 experience ketosis within 1-2 wk characterized by a 3- to 4-fold elevation in blood BHB levels, and exhibit  
465 greater energy expenditure and weight loss compared to humans on a low-fat, plant-based diet that contains  
466 10% fat and 75% carbohydrates (71). Likewise, KD-fed mice do not gain weight, but show enhanced energy  
467 expenditure after 5 wk of diet administration, and a trend toward weight loss during 9 wk of diet exposure,  
468 compared to mice fed a standard chow diet (72). Thus, neither weight gain or the obesity paradox are  
469 confounding features for the data we present here showing that both KD and dietary PA mediate innate  
470 immune memory *in vivo* during endotoxemia.

471 Further, the metabolism of dietary SFAs is a key element of immune system function, and metabolic  
472 intermediates enhanced by SFAs and PA alone, such as ceramide, serve as signaling lipids in diseases of  
473 inflammation (73). Mechanistically, we show that inhibiting ceramide synthesis or diverting metabolism away  
474 from ceramide synthesis using OA protects macrophages from PA-induced trained immunity, suggesting that  
475 dietary intervention may help regulate inflammatory dysregulation during disease (Fig 5). And, to complement

our *in vitro* mechanistic findings we show that 3 single i.p. injections of OA prior to endotoxin stimulation protects KD-fed mice from enhanced disease severity and mortality (Fig 5).

Our findings align with the growing body of evidence indicating that trained immunity is a double-edged sword, where the phenomenon can be beneficial for resistance to infection, but detrimental in the context of diseases exacerbated by systemic inflammation (74). Specifically, we show that PA-induced memory is beneficial in that it promotes clearance of *C. albicans* infection in the kidneys of *Rag1<sup>-/-</sup>* mice (Fig 4I). In stark contrast, PA-induced memory is detrimental in the context of endotoxemia, a disease driven by organ damage due to acute hyper-inflammation (75-79) (Fig 4G, H). Further, it is known that trained immunity is a key feature of BCG vaccination, which has been shown to enhance resistance to infections, and is a possible mechanism that drives increased resistance to severe COVID-19 in the BCG vaccinated population (7, 80). Thus, future research in understanding the plasticity of the SFA- and PA-regulated immune memory responses, enhanced pathogen clearance, and the mechanisms that drive this phenomenon, will be of interest to the larger medical community.

Mechanistically, it is appreciated that PA is not acting as a ligand for the pattern recognition receptor (PRR) TLR4, however the presence of TLR4 (independent of TLR4 signaling capability) is required for PA-dependent inflammation (14). Our data and others contribute to the growing evidence that PA is inducing cell intrinsic stress through alterations in metabolism. The crosstalk between glycolytic and oxidative metabolism, and epigenetics, is crucial for trained immunity in human monocytes, and metabolic intermediates of the TCA cycle directly modify histone methylation patterns associated with proinflammatory cytokines upregulated in trained immunity (4, 81, 82). While ceramides are known to modify histone acetylation and DNA methylation patterns (83), the interplay between ceramide metabolism and epigenetics within innate immune cells has not been explored. Though we have shown that PA-dependent ceramide production leads to innate immune memory, the impact of these alterations on the epigenome remains unknown. Therefore, the influence of ceramide metabolism on epigenetics will be important to consider in future trained immunity studies where PA serves as the primary stimulus.

Interestingly, we find here that immunoparalysis, which is associated with a prolonged septic response and is enhanced in patients with poorer outcomes, is greater in mice fed diets enriched in SFAs (Fig 1) (37, 38). However, we found that this SFA-dependent enhanced immunoparalysis is abrogated in germ-free mice,

504 suggesting, for the first time, that the microbial species within the SFA-fed mice may be regulating the late  
505 immunoparalytic phase of endotoxin shock. Considering the clinical correlation of immunoparalysis and  
506 increased sepsis mortality, it will be imperative to explore the identity of the SFA-dependent microbiome and  
507 the host/microbe mechanisms that drive sepsis-associated immunoparalysis.

508 Importantly, previous seminal studies concluded that mice treated with antibodies to the TNF receptor  
509 and challenged with systemic LPS increased survival from 0% to nearly 100%, suggesting that acute  
510 inflammation driven by TNF is responsible for endotoxemia-related mortality (75, 76). Further, it has been  
511 shown that TNF is required for acute renal failure (77), lung injury (78), and liver damage (79) during LPS  
512 challenge. These data show that acute inflammation, specifically the bioactivity of TNF, drives endotoxemia  
513 mortality and organ damage in conventional mice. It has also been shown that acute inflammation, specifically  
514 TNF production, is a driver of endotoxemia in GF mice (84). Thus, although our conventional mice show  
515 increased immunoparalysis, we suggest that early acute systemic inflammation is the driver of disease severity  
516 and mortality in both our conventional and GF endotoxemia mouse models; however, the data we present here  
517 is not sufficient to make this conclusion.

518 In conclusion, this unappreciated role of dietary SFAs, specifically PA, may provide insight into the  
519 long-lasting immune reprogramming associated with a high-SFA fed population, and lends insight into the  
520 complexity of nutritional immunoregulation. Considering the results in this study, we suggest the potential for  
521 SFAs such as PA to directly impact innate immune metabolism and epigenetics associated with inflammatory  
522 pathways. Thus, our findings are paramount not only for potential dietary interventions, but also treatment of  
523 inflammatory diseases exacerbated by metabolic dysfunction in humans.

## 525 **Materials and Methods**

526 **Cell lines and reagents.** RAW 264.7 macrophages (from ATCC), CASP-1KO BMDMs, BMDMs and BMMs  
527 were maintained in DMEM (Gibco) containing L-glutamine, sodium pyruvate, and high glucose supplemented  
528 with 10% heat-inactivated fetal bovine serum (FBS; GE Healthcare, SH3039603). BMDMs were also  
529 supplemented with 10% macrophage colony-stimulating factor (M-CSF; M-CSF-conditioned media was  
530 collected from NIH 3T3 cells expressing M-CSF, generously provided by Denise Monack at Stanford  
531 University).

**Generation of BMDMs, BMMs, and splenocytes.** Bone marrow-derived macrophages (BMDMs) and bone marrow-derived monocytes (BMMs) were harvested from the femurs and tibias of age-matched (6-8 wk) CO<sub>2</sub>-ethanized female BALB/c mice or male and female C57BL/6J mice. BMDM media was supplemented with 10% macrophage colony-stimulating factor (M-CSF) for differentiation, cells were seeded at  $5 \times 10^6$  in petri dishes and cultured for 6 days, collected with cold PBS, and frozen in 90% FBS and 10% DMSO in liquid nitrogen for later use. BMMs were isolated from BMDM fraction using EasySep™ Mouse Monocyte Isolation Kit (STEMCELL). Spleens were harvested from age-matched (6-8 wk) CO<sub>2</sub>-ethanized female BALB/c mice, tissue was disrupted using the end of a syringe plunger on a 70 μm cell strainer and rinsed with FACS buffer (PBS + 2mM EDTA). Cells were subjected to red blood cell lysis with RBC lysing buffer (Sigma) followed by neutralization in FACS buffer.

**Treatments.** After thawing and culturing for 5 days, BMDMs were pelleted and resuspended in DMEM containing 5% FBS, 2% endotoxin- and fatty acid-free bovine serum albumin (BSA; Proliant Biologicals) and 10% M-CSF. Cells were seeded at  $2.5 \times 10^5$  cells/well in 24-well tissue-culture plates, treated with EtOH (1.69%, or 0.83%) 10 ng/mL LPS (Ultrapure LPS, *E. coli* 0111:B4, Invivogen), 500 μM or 1 mM palmitic acid (Sigma-Aldrich, PHR1120), 10uM Fumonisin B1 (Sigma-Aldrich, F1147), or 200 μM oleic acid (Sigma-Aldrich, O7501). and incubated at 37°C and 5% CO<sub>2</sub> for 12 or 24 h. Next, cells were treated with an additional 10 ng/mL LPS, and incubated an additional 12 or 24 h. RAW 264.7 macrophages were thawed and cultured for 3-5 days, pelleted and resuspended in DMEM containing 5% FBS and 2% endotoxin- and fatty acid-free BSA, and treated identical to BMDM treatments. BMMs were seeded immediately after harvesting at  $4 \times 10^5$  cells/well in 96-well V-bottom plates in DMEM containing 10% FBS, and treated with LPS for 2 or 24 h. Splenocytes were seeded immediately after harvesting at  $1 \times 10^5$  cells/well in 96-well V-bottom plates in RPMI media with L-glutamine (Cytiva) containing 10% FBS, and treated with LPS for 2 or 24 h. BMDMs for *ex vivo* treatments were isolated as described above, plated at  $2.5 \times 10^5$  cells/well in 24-well plates, and stimulated with 10 ng/mL LPS after 12 h of adherence. For all treatments, supernatant was removed for ELISA analysis, and cells were lysed with TRizol (ThermoFisher), flash-frozen in liquid nitrogen, and stored at -80°C until qRT-PCR analysis. For all plates, all treatments were performed in triplicate.

560  
561 **Flow Cytometry.** Modified panel using combined methods from Kaufmann et al., Nowlan et al., and Vasquez  
562 et al. Red blood cells were lysed in BM cells using RBC lysis buffer (Biolegend). BM cells ( $3 \times 10^6$  cells) were  
563 stained with viability stain Live/Dead Fixable Aqua (ThermoFisher) at the concentration of 1:200 for 30 minutes  
564 at 4°C. Next, cells were washed with FACS buffer (PBS supplemented with 0.5% BSA; Proliant Biologicals,  
565 fatty acid free), and incubated with anti-CD16/32 (clone 93, BioLegend) at a concentration of 1:100 in FACS  
566 buffer for 10 minutes at 4°C. The following antibodies were then used for staining HSCs, and MPPs: anti-Ter-  
567 110, anti-CD11b (clone M1/70), anti-CD5 (clone 53-7.3), anti-CD4 (clone RM4-5), anti-CD8a (clone 53-6.7),  
568 anti-CD45R (clone RA3-6B2), and anti-Ly6G/C (clone RB6-8C5), all biotin-conjugated (all BD Bioscience),  
569 were added at a concentration of 1:100 for 30 minutes at 4°C, and washed with FACS buffer. Streptavidin-  
570 APC-Cy7 (eBioscience), anti-CD150-eFluor450 (clone Q38-480, eBioscience), anti-CD48-PerCPeFluor710  
571 (BD Bioscience), anti-Flt3-PE (clone A2F10.1, BD Bioscience), anti-CD34-PEDazzle 594 (clone HM34,  
572 BioLegend), anti-CD27-PE-Cy7 (eBioscience), and anti-CD201-APC (eBioscience) were added all at a  
573 concentration of 1:100 for 20 minutes at 4°C. All cells were then washed with FACS buffer before and after  
574 incubation in 1% paraformaldehyde for 30 minutes at 4°C. Cells were acquired on BD flow cytometer  
575 (FACSymphony A1 Cell Analyzer) with FACSDiva Software. Analyses were performed using FlowJo software  
576 v.10.1. The DownSample version 3.3.1 plugin was used to standardize events for each sample after  
577 populations were gated.

578  
579 **Lactate dehydrogenase (LDH) assays.** BMDMs were cultured as stated above with culture media, PA, or  
580 ethanol in 96-well tissue-culture plates at a concentration of  $5 \times 10^4$  cells/well and incubated for 12 hours. Cells  
581 were treated with PBS or 10 ng/mL LPS in a phenol-red-free Optimem media (ThermoFisher) and incubated  
582 an additional 12 or 24 h. Supernatants were collected at the specified time points with LDH release quantified  
583 with a CytoTox96 Non-Radioactive Cytotoxicity Assay (Promega). Cytotoxicity was measured per well as a  
584 percentage of max LDH release, with background media-only LDH release subtracted. For all plates, all  
585 treatments were performed in triplicate.

586

587 **Measurement of cell viability.** Cell viability was determined by 0.4% Trypan Blue dye exclusion test executed  
588 by a TC20 Automated Cell Counter (Bio-Rad).

589  
590 **Blood RNA extraction and real-time qPCR.** Mice were treated with PBS or LPS, and at specified time points  
591 10-20  $\mu$ L of blood was collected from the tail vein, transferred into 50  $\mu$ L of RNALater (ThermoFisher Scientific)  
592 and frozen at  $-80^{\circ}\text{C}$ . RNA extractions were performed using RNeasy Mini Kit (Qiagen) and cDNA was  
593 synthesized from RNA samples using SuperScript III First-Strand synthesis system (Invitrogen). Gene specific  
594 primers were used to amplify transcripts using SsoAdvanced Universal SYBR Green Supermix (Bio-Rad). A  
595 complete list of all primers used, including the names and sequences, is supplied as Supplementary File 2.

596  
597 **Enzyme-linked immunosorbent assay (ELISA).** TNF, IL-6, and IL-1 $\beta$  concentrations in mice serum were  
598 measured and analyzed using TNF, IL-6, and IL-1 $\beta$  Mouse ELISA Kits (ThermoFisher Scientific), according to  
599 the manufacturer's instructions. Absorbances were measured at a wavelength of 450 nm using a microplate  
600 reader (BioTek Synergy HTX). Values below the limit of detection (LOD) of the ELISA were imputed with LOD  
601 divided by 2 (LOD/2) values.

602  
603 **LPS-induced endotoxemia model.** Age-matched (6 – 8 wk) female BALB/c mice were anesthetized with  
604 isoflurane and injected subcutaneously with ID transponders (Bio Medic Data Systems). 2 wk post diet change,  
605 and 1 wk post ID transponder injection, mice were stimulated with a single injection of 6-10 mg/kg LPS  
606 reconstituted in endotoxin-free LAL reagent water (Invivogen) and diluted in PBS for a total volume of 200  $\mu$ L.  
607 Control mice received corresponding volumes of PBS. Progression of disease was monitored every 2 h after  
608 LPS injection for clinical signs of endotoxin shock based on weight, coat and eyes appearance, level of  
609 consciousness and locomotor activity. Age-matched (20 – 21 wk) female C57BL/6 mice were treated as  
610 described above, except for their LPS dose (4.5 mg/kg). Temperature was recorded using a DAS-8007  
611 thermo-transponder wand (Bio Medic Data Systems). For PA injections, a solution of 750 mM ethyl palmitate  
612 (Millipore Sigma), 1.6% lecithin (Sigma-Aldrich) and 3.3% glycerol was made in endotoxin-free LAL reagent  
613 water (Lonza). The lecithin-glycerol-water solution was used as a vehicle, and mice were injected with 200  $\mu$ L  
614 of the vehicle as a control, or ethyl palmitate solution to increase serum PA levels. For OA injections, a solution



615 of 300 mM OA (Sigma-Aldrich) was made using the same solution and vehicle described above. Mice were  
616 injected i.p. with 200  $\mu$ L of the vehicle as a control, or OA solution, between 7 – 9 pm for 3 d prior to LPS  
617 exposure.

618  
619 **Mouse diets, glucose, and ketones.** Six-week-old female mice were fed soft, irradiated chow (PicoLab  
620 Mouse Diet 20, product 5058) and allowed to acclimate to research facility undisturbed for one week. Chow  
621 was replaced by Western Diet (Envigo, TD.88137), Ketogenic Diet (Envigo, TD.180423), or Standard Chow  
622 (Envigo, TD.08485) and mice were fed *ad libitum* for two weeks before induction of endotoxemia. For  
623 Ketogenic Diet, food was changed daily. For Western Diet, food was changed every 72 hours. Ketones and  
624 blood glucose were measured weekly and immediately prior to LPS injections with blood collected from the tail  
625 vein using Blood Ketone & Glucose Testing Meter (Keto-Mojo), or with urine collected on ketone indicator  
626 strips (One Earth Health, Ketone Test Strips).

627  
628 **Statistics analysis.** Mann Whitney, Mantel-Cox, and student's t-tests were carried out with GraphPad Prism  
629 9.0 software.

630  
631 **Ethical approval of animal studies.** All animal studies were performed in accordance with National Institutes  
632 of Health (NIH) guidelines, the Animal Welfare Act, and US federal law. All animal experiments were approved  
633 by the Oregon Health and Sciences University (OHSU) Department of Comparative Medicine or Oregon State  
634 University (OSU) Animal Program Office and were overseen by the Institutional Care and Use Committee  
635 (IACUC) under Protocol IDs #IP00002661 & IP00001903 at OHSU and #5091 at OSU. Conventional animals  
636 were housed in a centralized research animal facility certified by OHSU. Conventional 6-10 wk-aged female  
637 BALB/c mice (Jackson Laboratory 000651) were used for the endotoxemia model, and isolation of BMDMs,  
638 BMMs, and splenocytes. GF male and female C57BL/6 mice (Oregon State University; bred in house) between  
639 14 and 23 wk old were used for the GF endotoxemia model. BALB/c *Rag1<sup>-/-</sup>* mice between 8 and 24 wk were  
640 infected i.v. with  $2 \times 10^6$  CFUs of *C. albicans* SC5314 (ATCC #MYA-2876) and kidney fungal burden was  
641 assessed 24 h post-infection. Kidneys were harvested 24 h post-infection and homogenized organs were  
642 plated in serial dilutions on Yeast Peptone Dextrose plates to assess fungal burden.

## Lipidomics PCA Analysis

Mice on specialized diets were sacrificed at the indicated time points after PBS or LPS treatment with 300-600 $\mu$ L of blood collected via cardiac puncture into heparinized tubes. Blood samples were centrifuged for 15 minutes at 2,500rpm at 4°C and serum was transferred to a new tube before storage at -80°C. Serum samples were analyzed via LC-MS/MS. Lipidomic data sets were scaled using the *scale* function and principal component analyses were performed using the *prcomp* function from the stats package in R Version 3.6.2. Visualization of PCAs and biplots was performed with the *fviz\_pca\_ind* and *fviz\_pca\_biplot* functions from the factoextra package and with the *ggplot2* package (85, 86). For each diet group, 95% confidence ellipses were plotted around the group mean using the *coord.ellipse* function from the FactoMineR package (87). Heatmaps were created using the *pheatmap* package (88).

## Acknowledgements

We would like to thank Ajesh Saini, a student in the Napier Lab, for his contributions in carrying out the ELISA data within this manuscript. This study was supported by National Institute of General Medical Sciences (NIGMS) grant 5R35GM133804-02 to B.A.N.

## Figure Legends

**Fig. 1 Diets enriched in SFAs lead to enhanced endotoxemia severity and altered systemic inflammatory profiles, independent of diet-associated microbiome. (A-G)** Age-matched (6 – 8 wk) female BALB/c mice were fed SC, WD, or KD for 2 wk and injected i.p. with 6 mg/kg of LPS. **(A)** Temperature loss and **(B)** survival were monitored every 2 h. At indicated times 10 – 20  $\mu$ L of blood was drawn via the tail vein, RNA was collected, and samples were assessed for expression of **(C)** *Tnf*, **(D)** *Il6*, **(E)** *Il1b*, and **(F)** *Il10* via qRT-PCR. **(G)** *Il10:Tnf* ratio was calculated for 5, 10, 15, and 20 hours p.i. with LPS. **(H-N)** Next, 19 – 23 wk old female and 14 – 23 wk old male and female germ-free C57BL/6 mice were fed SC, WD, or KD for 2 wk and injected i.p. with 50 mg/kg of LPS. **(H)** Temperature loss and **(I)** survival were monitored every 5 h p.i. **(J-N)** At indicated times, 10-20  $\mu$ L of blood was drawn via the tail vein, RNA was collected, and samples were assessed for expression of **(J)** *Tnf*, **(K)** *Il6*, **(L)** *Il1b*, and **(M)** *Il10* via qRT-PCR. **(N)** *Il10:Tnf* ratio was calculated

for 5 and 10 h p.i. with LPS. For **A-G**,  $n = 5$  per diet group, and data are representative of 1 experiment. For **H-N**, SC,  $n = 6$ ; WD,  $n = 5$ , and KD,  $n = 9$ , and data are representative of 1 experiment. For **A, C-G, H**, and **J-N** a Mann Whitney test was used for pairwise comparisons. For **B** and **I** a log-rank Mantel-Cox test was used for survival curve comparison. For all panels,  $*p < 0.05$ ;  $**p < 0.01$ ;  $***p < 0.001$ . For **C-E**,  $\Phi$  symbols indicate WD significance and  $\infty$  symbols indicate KD significance. Error bars shown mean  $\pm$  SD.

**Fig. 2 KD feeding alters HSC populations and BMDMs from KD-fed mice show a hyper-inflammatory response to LPS *ex vivo*.** Bone marrow was extracted from the femurs and tibias of age-matched (6 – 8 wk) female BALB/c mice fed SC, WD, or KD for 2 wk. **(A)** FACS plots of total HSCs ( $CD201^+CD27^+$ ) and **(B)** LT-HSCs, ST-HSCs, and MPPs from mice fed SC, WD, or KD for 2 wk. Quantification of **(C)** the total numbers of LT- and ST-HSCs, and MPPs in BM from mice fed SC, WD, or KD for 2 wk. Next, BMDMs were plated at  $5 \times 10^6$  cells/mL, and differentiated for 7 d in media supplemented with M-CSF. Cells were split and plated in 24-well plates to adhere for 12 h, and treated with media (Ctrl) or LPS (24 h; 10 ng/mL). Supernatants were assessed via ELISA for **(D)** TNF and **(E)** IL-6 secretion at 24 h post-LPS treatment. IL-6 Ctrl supernatants were below the limit of detection; ND = no data. **(C)** a Mann Whitney test was used for pairwise comparisons. **(D, E)** For all plates, all treatments were performed in triplicate, and a student's t-test was used for statistical significance. \*,  $p < 0.05$ ; \*\*,  $p < 0.01$ ; \*\*\*,  $p < 0.001$ ; \*\*\*\*,  $p < 0.0001$ . Error bars show the mean  $\pm$  SD.

**Fig. 3 KD alters lipid profiles and PA is mediating a hyper-inflammatory response to secondary challenge with LPS.** Data points represent single animal samples and colors represent groups fed SC (grey) or KD (orange) diets for two weeks. A 95% confidence ellipse was constructed around the mean point of each group for **(A)** free fatty acids (FFA), **(B)** triglycerides (TAG), and **(C)** phosphatidylcholines (PC). **(D)** Heatmap analysis of free fatty acids in SC and KD mice. Components that are significantly different between the two groups are in bold. Below the heatmap is a comparison of palmitic acid 16:0 peak area detected by LC-MS/MS between SC and KD groups; AUC = area under the curve. Statistical significance is determined by unpaired two-tailed t-test between SC and KD groups with  $n=3$  per group. Primary bone marrow-derived macrophages (BMDMs) were isolated from aged-matched (6 – 8 wk) C57BL/6 female and male mice. BMDMs were plated at  $1 \times 10^6$  cells/mL and treated with either ethanol (EtOH; media with 0.83% ethanol), media (Ctrl for LPS), or LPS

(10 ng/mL) for 12 h, or palmitic acid (PA stock diluted in 0.83% EtOH; 1 mM PA conjugated to 2% BSA) for 12 h, with and without a secondary challenge with LPS. After indicated time points, RNA was isolated and expression of **(E)** *Tnf*, **(F)** *Il6*, **(G)** *Il1b* was measured via qRT-PCR. BMDMs were plated at  $1 \times 10^6$  cells/mL and treated with either ethanol (EtOH; media with 0.83% ethanol), media (Naïve), or 1 mM PA for 12 h followed by PBS (control) or LPS (10 ng/mL). Supernatants were assessed via ELISA for **(H)**, TNF, **(I)** IL-6, and **(J)** IL-1 $\beta$  secretion. Next, BMDMs were plated at  $1 \times 10^6$  cells/mL and treated with either media (Ctrl), LPS (10 ng/mL) for 24 h, palmitic acid (PA stock diluted in 0.83% EtOH; 0.5 mM PA conjugated to 2% BSA) for 12 h, Fumonisin B1 (FB1; 10  $\mu$ M; diluted in 0.14% EtOH) or EtOH (0.97% to mimic simultaneous PA/FB1 treatment). Controls for all treatments are shown next to experimental groups treated additionally with LPS (10 ng/mL) for 24 h. Supernatants were assessed via ELISA for **(K)**, TNF, **(L)** IL-6, and **(M)** IL-1 $\beta$  secretion. For all plates, all treatments were performed in triplicate. For all panels, a student's t-test was used for statistical significance. \*,  $p < 0.05$ ; \*\*,  $p < 0.01$ ; \*\*\*,  $p < 0.001$ ; \*\*\*\*,  $p < 0.0001$ . Error bars show the mean  $\pm$  SD.

**Fig. 4 PA acts as a novel mediator of trained immunity by inducing a hyper-inflammatory response LPS-induced endotoxemia, and enhancing clearance of *Candida albicans* infection.** Age-matched (6 – 8 wk) female BALB/c mice were fed SC for 2 wk and injected i.p. with ethyl palmitate (PA, 750 mM) or vehicle (Veh) solutions 12 h before i.p. LPS injections (10 mg/kg). **(A)** Temperature loss was monitored every 2 h as a measure of disease severity or **(B)** survival. At indicated times blood was collected via the tail vein, RNA was extracted, and samples were assessed for expression of **(C)** *Tnf*, **(D)** *Il6*, and **(E)** *Il1b* via qRT-PCR. **(F)** Blood was collected via the tail vein from Vehicle (Veh) and PA pre-treated (12 h PA) mice immediately prior to LPS injection and samples were assessed for expression of *Tnf*, *Il6*, *Il1b*, and *Il10* via qRT-PCR. Additionally, age-matched (6 – 8 wk) female BALB/c mice fed SC, injected i.p. with ethyl palmitate (PA, 750 mM) or vehicle (Veh) solutions every day for 9 days, and then rested for 7 d before i.p. LPS injections (10 mg/kg) **(G)** Temperature loss and **(H)** survival were monitored during endotoxemia. **(I)** Age-matched (8-9 wk) female *Rag1*<sup>-/-</sup> mice were injected i.p. with ethyl palmitate (PA, 750 mM) or vehicle (Veh) solutions 12 h before i.v. *C. albicans* infection. Fungal burden of kidneys from Vehicle (Veh) and PA pre-treated (12 h PA) mice 24 h after *C. albicans* infection. For **(A-F)**, experiments were run 3 times and data are representative of 1 experiment,  $n=3$  mice/group. For **(G, H)**, experiments were run twice, and data are representative of 1 experiment. For

Veh→SC, n=3 mice and PA→SC, n=5 mice. For **(I)**, experiments were run 3 times and data are representative of 1 experiment, n=6 mice/group. For **(A)**, **(C-E)**, **(G)** and **(I)**, a Mann Whitney test was used for pairwise comparisons. For **(B)** and **(H)**, a log-rank Mantel-Cox test was used for survival curve comparison. For all panels, \*,  $p < 0.05$ ; \*\*,  $p < 0.01$ ; \*\*\*,  $p < 0.001$ ; \*\*\*\*,  $p < 0.0001$ . Error bars shown mean  $\pm$  SD.

**Fig. 5 Oleic acid reverses PA-dependent hyper-inflammation in response to LPS *in vitro*, and PA-dependent enhanced endotoxemia disease severity *in vivo*.** Primary bone marrow-derived macrophages (BMDMs) were isolated from aged-matched (6 – 8 wk) C57BL/6 female and male mice. BMDMs were plated at  $1 \times 10^6$  cells/mL and treated with either media (Ctrl), LPS (10 ng/mL) for 24 h, palmitic acid (PA stock diluted in 0.83% EtOH; 0.5 mM PA conjugated to 2% BSA) for 12 h, or oleic acid (OA; 200  $\mu$ M; diluted in endotoxin-free water). Controls for all treatments are shown next to experimental groups treated additionally with LPS (10 ng/mL) for 24 h. Supernatants were assessed via ELISA for **(A)** TNF, **(B)** IL-6, and **(C)** IL-1 $\beta$  secretion. Age-matched (6 – 8 wk) female BALB/c mice were fed SC or KD for 2 wk and injected i.p. with 7 mg/kg LPS or **(D)** Temperature loss and **(E)** survival were monitored every 2 h. For **(A-C)**, a student's t-test was used for statistical significance. For **(D)**, a Mann Whitney test was used for pairwise comparisons. For **(E)**, a log-rank Mantel-Cox test was used for survival curve comparison. For **(D, E)**, experiments were run 3 times and data are representative of 1 experiment, n=5 mice/group.  $\beta$  symbols indicate KD+Veh vs KD+OA significance, and  $\infty$  symbols indicate KD+Veh vs. SC+ Veh. For all panels, \*,  $p < 0.05$ ; \*\*,  $p < 0.01$ ; \*\*\*,  $p < 0.001$ ; \*\*\*\*,  $p < 0.0001$ . Error bars shown mean  $\pm$  SD.

### Supplementary Figure Legends

**Figure 1 Supplementary Figure 1. Increase in disease severity in KD mice is independent of ketosis.** Age-matched (6 – 8 wk) female BALB/c mice were fed SC, WD, or KD for 2 wk. At 1 wk and 2 wk, **(A)** blood was collected via the tail vein to measure blood glucose levels using a glucose testing meter (Keto-Mojo) and **(B)** urine was collected on ketone indicator strips to measure levels of systemic acetoacetate (AcAc). Age-matched (6 – 8 wk) female BALB/c mice were fed SC supplemented with 1,3-butanediol (SC + BD) or with a saccharine vehicle solution as a control (SC + Veh), or KD for 2 wk. At 1 wk and 2 wk, **(C)** blood was collected via the tail vein to measure levels of systemic  $\beta$ -hydroxybutyrate (BHB) using a ketone testing meter (Keto-

755 Mojo). At 2 wk, SC-, WD-, and KD-fed mice were injected i.p. with LPS (6 mg/kg) and **(D)** 25 h p.i. blood  
756 glucose levels were measured as stated in **A**. **(E)** temperature loss and **(F)** survival were monitored every 2 h  
757 for mice treated as in **C** followed by i.p. injection with LPS (10 mg/kg). Age-matched (20-21 wk) female  
758 C57BL/6 mice were fed SC, WD, or KD for 2 wk followed by i.p. injection with LPS (4.5 mg/kg). **(G)**  
759 temperature loss and **(H)** survival were monitored every 2 h. For **(A, B, D)** all experiments were run 3 times  
760 and data are representative of 1 experiment, n = 5-8 mice/group. For **(C, E, F)** all experiments were run 3  
761 times and data are representative of 1 experiment, n = 5-8 mice/group. For **(G, H)** data are representative of 1  
762 experiment, n = 10 mice/group. For **(A-C, E, G)** a Mann-Whitney U test was used for pairwise comparisons.  
763 For **(F, H)** a log-rank Mantel-Cox test was used for survival curve comparison. For **(E)**  $\beta$  symbols indicate SC +  
764 Veh vs. SC + BD significance,  $\infty$  symbols indicate SC + Veh vs. KD significance, and  $\delta$  symbols indicate SC +  
765 BD vs. KD significance. For **(G)**  $\phi$  symbols indicate SC vs. WD significance, and  $\infty$  symbols indicate SC w. KD  
766 significance. For all panels, \* p < 0.05; \*\* p < 0.01; \*\*\* p < 0.001; \*\*\*\* p < 0.0001. Error bars show mean  $\pm$  SD.

767  
768 **Figure 2 Supplementary Figure 1. KD does not alter MPP differentiation or basal inflammation in**  
769 **BMDMs, and monocytes and splenocytes show a hyper-inflammatory response to LPS ex vivo.** Age-  
770 matched (6 – 8 wk) conventional, wild-type, female BALB/c mice were fed SC, WD, or KD for 2 wk. Bone  
771 marrow was extracted from the femurs and tibias of mice, HSCs were isolated via FACS and **(A)** MPPs were  
772 quantified. BMDMs were plated at  $5 \times 10^6$  cells/mL, and differentiated for 7 d in media supplemented with M-  
773 CSF. Cells were split and plated in 24-well plates to adhere for 12 h, and treated with media (Ctrl) for 24 h.  
774 Supernatants were assessed via ELISA for **(B)** TNF and IL-6 secretion. Monocytes were isolated from the  
775 femurs and tibias of mice and plated at  $2 \times 10^6$  cells/mL. RNA was extracted from **(C)** untreated monocytes (0 h)  
776 or **(D)** monocytes with LPS (10 ng/mL) for 2 h. Expression of *Tnf* and *Il6* was analyzed via qRT-PCR.  
777 Splenocytes were isolated and plated at  $1 \times 10^6$  cells/mL. RNA was isolated from **(E)** untreated splenocytes (0 h)  
778 or **(F)** splenocytes treated with LPS (10 ng/mL) for 2 h. Expression of *Tnf* and *Il6* was analyzed via qRT-PCR. n  
779 = 3 mice/group in each representative experiment. A student's t-test was used for statistical significance. For  
780 all panels, \* p < 0.05; \*\* p < 0.01; \*\*\* p < 0.001; \*\*\*\* p < 0.0001. Error bars show mean  $\pm$  SD.

**Figure 2 Supplementary Figure 2. Gating strategy for HSCs, related to Figures 2 and 4.** Cells were gated in FSC-A against SSC-A. Doublets were excluded using FSC-A against FSC-H and subsequently SSC-A against SSC-H. Viable cells were gated and lineage-committed cells were excluded. Within the lineage-negative cells, the CD201<sup>+</sup>CD27<sup>+</sup> population was gated. In a CD150 against CD48 plot, the CD201<sup>+</sup>CD27<sup>+</sup> cells were divided into LT-HSC, ST-HSC, MPP, and the remaining CD150<sup>-</sup>CD48<sup>-</sup> population. MPPs were characterized as MPP3 and MPP4 by their surface expression of CD34 and Flt3.

**Figure 3 Supplementary Figure 1. Principal component analysis (PCA) and heatmap analysis of sphingolipid lipidomic data in mouse serum samples. (A)** Data points represent single animal samples and colors represent groups fed SC (grey) or KD (orange) diets for two weeks and a 95% confidence ellipse was constructed around the mean point of each group. Heatmap analysis of **(B)** sphingolipids (SM), **(C)** triglycerides (TG), and **(D)** phosphatidylcholines (PC) in SC and KD groups. Lipid components containing 16:0 palmitic chains are highlighted in purple and components that are significantly different between the two groups are in bold. Statistical significance determined by unpaired two-tailed t-test between SC and KD groups. \* p < 0.05; \*\* p < 0.01; \*\*\* p < 0.001; \*\*\*\* p < 0.0001. n=3 per group.

**Figure 3 Supplementary Figure 2. Physiological levels of Palmitic Acid induce a hyper-inflammatory response to secondary challenge with LPS in macrophages.** Primary bone marrow-derived macrophages (BMDMs) were isolated from age-matched (6 – 8 wk) female and male mice. **(A-C)** BMDMs were plated at 1x10<sup>6</sup> cells/mL and treated with ethanol (EtOH; media with 1.69% ethanol), media (Ctrl for LPS), or palmitic acid (PA, 1 mM; diluted in 1.69% EtOH) for 12 h. Next, PA-treated cells were treated with LPS (10 ng/mL) for 24 h, and all other wells were given fresh media. **(D-I)** BMDMs were plated at 1x10<sup>6</sup> cells/mL and treated with PA (0.5 mM; diluted in 1.69% EtOH) for 12 or 24 h. Next, PA-treated cells were treated with LPS (10 ng/mL) for 24 h, and all other wells were given fresh media. After indicated time points, RNA was isolated and expression of **A, D, G** *Tnf*, **B, E, H** *Il6*, and **C, F, I** *Il1b* was measured via qRT-PCR. For all plates treatments were performed in triplicate. For all panels, a student's t-test was used for statistical significance. \* p < 0.05; \*\* p < 0.01; \*\*\* p < 0.001; \*\*\*\* p < 0.0001. Error bars show mean ± SD.

**Figure 3 Supplementary Figure 3. Cytotoxicity as determined by LDH release from BMDMs pre-treated with PA followed by LPS stimulation.** BMDMs from age-matched (6 – 8 wk) male and female C57BL/6 mice were plated in 96-well plates at  $5 \times 10^4$  cells/well and incubated for 12 h with PA (0.5 mM or 1 mM). Next, media was removed, and cells were treated with PBS for 10 ng/mL LPS in phenol-red-free Opti-MEM media and incubated for an additional 24 h. Supernatants were collected and LDH release was quantified using CytoTox96 Non-Radioactive Cytotoxicity Assay. **(A, B)** Cytotoxicity is shown as percentage of max LDH release. For all plates all treatments were performed in triplicate, and a student's t-test was used for statistical significance. \*  $p < 0.05$ ; \*\*  $p < 0.01$ ; \*\*\*  $p < 0.001$ ; \*\*\*\*  $p < 0.0001$ . Error bars show mean  $\pm$  SD.

**Figure 4 Supplementary Figure 1. Palmitic acid i.p. injections enhance serum PA concentrations and PA-induced trained immunity is time-dependent.** Conventional wild-type, age-matched (6 – 8 wk), female BALB/c mice were fed SC for 2 wk and injected i.p. with ethyl palmitate (PA 750 mM in 1.6% lecithin and 3.3% glycerol in endotoxin-free LAL reagent water) or a vehicle solution (Veh, 1.6% lecithin and 3.3% glycerol in endotoxin-free LAL reagent water). **(A)** serum was collected via cardiac punctures from mice 2 h and 5 h p.i. Serum samples were analyzed for absolute PA concentrations using qualitative tandem liquid chromatography quadrupole time of flight mass spectrometry (LC-QToF MS/MS). At 0, 3, and 6 h after PA injection, endotoxemia was induced via a single i.p. injection of LPS (10 mg/kg). **(B)** Temperature loss and **(C)** survival were monitored every 2 h. **(D)** blood was collected via the tail vein to measure blood glucose levels at 0 and 20 h p.i. with LPS using a glucose testing meter (Keto-Mojo). For **(D)** a Mann Whitney test was used for pairwise comparisons. Data is representative of 1 experiment,  $n = 3-4$  mice/group. \*  $p < 0.05$ ; \*\*  $p < 0.01$ ; \*\*\*  $p < 0.001$ ; \*\*\*\*  $p < 0.0001$ . Error bars show mean  $\pm$  SD.

**Supplemental File 1. Diet compositions (values represent percentage of total kcal)**

**Supplemental File 2. List of primers used in this study**

**Figure 1 – Source data 1. Data and statistics for graphs depicted in Figure 1 A-N**

**Figure 2 – Source data 1. Data and statistics for graphs depicted in Figure 2 A-E**

**Figure 3 – Source data 1. Data and statistics for graphs depicted in Figure 3 A-M**

**Figure 4 – Source data 1. Data and statistics for graphs depicted in Figure 4 A-I**



838 **Figure 5 – Source data 1. Data and statistics for graphs depicted in Figure 5 A-E**

839 **Figure 1 – Figure Supplement 1 – Source data 1. Data for graphs depicted in Figure 1 – Figure**  
840 **Supplement 1 A-H**

841 **Figure 2 – Figure Supplement 1 – Source data 1. Data for graphs depicted in Figure 3 – Figure**  
842 **Supplement 1 A-F**

843 **Figure 3 – Figure Supplement 2 – Source data 1. Data for graphs depicted in Figure 3 – Figure**  
844 **Supplement 2 A-D**

845 **Figure 3 – Figure Supplement 3 – Source data 1. Data for graphs depicted in Figure 3 – Figure**  
846 **Supplement 3 A-B**

847 **Figure 4 – Figure Supplement 1 – Source data 1. Data for graphs depicted in Figure 4 – Figure**  
848 **Supplement 1 A-D**

849  
850 **References**

- 851 1. M. G. Netea *et al.*, Defining trained immunity and its role in health and disease. *Nat Rev Immunol* **20**,  
852 375-388 (2020).
- 853 2. J. Kleinnijenhuis *et al.*, Bacille Calmette-Guerin induces NOD2-dependent nonspecific protection from  
854 reinfection via epigenetic reprogramming of monocytes. *Proc Natl Acad Sci U S A* **109**, 17537-17542  
855 (2012).
- 856 3. J. Quintin *et al.*, *Candida albicans* infection affords protection against reinfection via functional  
857 reprogramming of monocytes. *Cell Host Microbe* **12**, 223-232 (2012).
- 858 4. S. Saeed *et al.*, Epigenetic programming of monocyte-to-macrophage differentiation and trained innate  
859 immunity. *Science* **345**, 1251086 (2014).
- 860 5. H. Lanz-Mendoza, J. Contreras-Garduno, Innate immune memory in invertebrates: Concept and  
861 potential mechanisms. *Dev Comp Immunol* **127**, 104285 (2022).
- 862 6. N. Katzmarski *et al.*, Transmission of trained immunity and heterologous resistance to infections across  
863 generations. *Nat Immunol* **22**, 1382-1390 (2021).
- 864 7. M. G. Netea *et al.*, Trained immunity: A program of innate immune memory in health and disease.  
865 *Science* **352**, aaf1098 (2016).

- 866 8. C. Covian, A. Retamal-Diaz, S. M. Bueno, A. M. Kalergis, Could BCG Vaccination Induce Protective  
867 Trained Immunity for SARS-CoV-2? *Front Immunol* **11**, 970 (2020).
- 868 9. D. K. Meena *et al.*, Beta-glucan: an ideal immunostimulant in aquaculture (a review). *Fish Physiol*  
869 *Biochem* **39**, 431-457 (2013).
- 870 10. M. van Splunter *et al.*, Induction of Trained Innate Immunity in Human Monocytes by Bovine Milk and  
871 Milk-Derived Immunoglobulin G. *Nutrients* **10**, (2018).
- 872 11. B. A. Swinburn *et al.*, The global obesity pandemic: shaped by global drivers and local environments.  
873 *Lancet* **378**, 804-814 (2011).
- 874 12. B. M. Popkin, Global nutrition dynamics: the world is shifting rapidly toward a diet linked with  
875 noncommunicable diseases. *Am J Clin Nutr* **84**, 289-298 (2006).
- 876 13. A. Christ, E. Latz, The Western lifestyle has lasting effects on metaflammation. *Nat Rev Immunol* **19**,  
877 267-268 (2019).
- 878 14. G. I. Lancaster *et al.*, Evidence that TLR4 Is Not a Receptor for Saturated Fatty Acids but Mediates  
879 Lipid-Induced Inflammation by Reprogramming Macrophage Metabolism. *Cell Metab* **27**, 1096-  
880 1110.e1095 (2018).
- 881 15. C. N. Lumeng, J. L. Bodzin, A. R. Saltiel, Obesity induces a phenotypic switch in adipose tissue  
882 macrophage polarization. *J Clin Invest* **117**, 175-184 (2007).
- 883 16. P. J. Meikle, S. A. Summers, Sphingolipids and phospholipids in insulin resistance and related  
884 metabolic disorders. *Nat Rev Endocrinol* **13**, 79-91 (2017).
- 885 17. A. W. B. Reyes *et al.*, Protection of palmitic acid treatment in RAW264.7 cells and BALB/c mice during  
886 *Brucella abortus* 544 infection. *Journal of Veterinary Science* **22**, (2021).
- 887 18. B. A. Napier *et al.*, Western diet regulates immune status and the response to LPS-driven sepsis  
888 independent of diet-associated microbiome. *Proc Natl Acad Sci U S A* **116**, 3688-3694 (2019).
- 889 19. A. Christ *et al.*, Western Diet Triggers NLRP3-Dependent Innate Immune Reprogramming. *Cell* **172**,  
890 162-175.e114 (2018).
- 891 20. J. D. Schilling *et al.*, Palmitate and Lipopolysaccharide Trigger Synergistic Ceramide Production in  
892 Primary Macrophages. *Journal of Biological Chemistry* **288**, 2923-2932 (2013).

- 893 21. Y. Zhang *et al.*, Adipose Fatty Acid Binding Protein Promotes Saturated Fatty Acid-Induced  
894 Macrophage Cell Death through Enhancing Ceramide Production. *J Immunol* **198**, 798-807 (2017).
- 895 22. M. Divangahi *et al.*, Trained immunity, tolerance, priming and differentiation: distinct immunological  
896 processes. *Nat Immunol* **22**, 2-6 (2021).
- 897 23. E. Kaufmann *et al.*, BCG Educates Hematopoietic Stem Cells to Generate Protective Innate Immunity  
898 against Tuberculosis. *Cell* **172**, 176-190 e119 (2018).
- 899 24. B. A. Napier *et al.*, Complement pathway amplifies caspase-11-dependent cell death and endotoxin-  
900 induced sepsis severity. *J Exp Med*, (2016).
- 901 25. H. Saito, E. R. Sherwood, T. K. Varma, B. M. Evers, Effects of aging on mortality, hypothermia, and  
902 cytokine induction in mice with endotoxemia or sepsis. *Mech Ageing Dev* **124**, 1047-1058 (2003).
- 903 26. C. F. Raetzsch *et al.*, Lipopolysaccharide inhibition of glucose production through the Toll-like receptor-  
904 4, myeloid differentiation factor 88, and nuclear factor kappa b pathway. *Hepatology* **50**, 592-600  
905 (2009).
- 906 27. J. P. Filkins, R. P. Cornell, Depression of hepatic gluconeogenesis and the hypoglycemia of endotoxin  
907 shock. *Am J Physiol* **227**, 778-781 (1974).
- 908 28. E. L. Goldberg *et al.*, Ketogenic diet activates protective  $\gamma\delta$  T cell responses against influenza virus  
909 infection. *Sci Immunol* **4**, (2019).
- 910 29. A. J. Lewis, C. W. Seymour, M. R. Rosengart, Current Murine Models of Sepsis. *Surg Infect (Larchmt)*  
911 **17**, 385-393 (2016).
- 912 30. A. Wang *et al.*, Opposing Effects of Fasting Metabolism on Tissue Tolerance in Bacterial and Viral  
913 Inflammation. *Cell* **166**, 1512-1525.e1512 (2016).
- 914 31. Y. V. Radzyukevich, N. I. Kosyakova, I. R. Prokhorenko, Participation of Monocyte Subpopulations in  
915 Progression of Experimental Endotoxemia (EE) and Systemic Inflammation. *Journal of Immunology*  
916 *Research* **2021**, 1-9 (2021).
- 917 32. L. Zhang *et al.*, Splenocyte Apoptosis and Autophagy Is Mediated by Interferon Regulatory Factor 1  
918 During Murine Endotoxemia. *Shock* **37**, 511-517 (2012).

- 919 33. E. A. Schwartz *et al.*, Nutrient modification of the innate immune response: a novel mechanism by  
920 which saturated fatty acids greatly amplify monocyte inflammation. *Arterioscler Thromb Vasc Biol* **30**,  
921 802-808 (2010).
- 922 34. C. Fang *et al.*, Differential regulation of lipopolysaccharide-induced IL-1beta and TNF-alpha production  
923 in macrophages by palmitate via modulating TLR4 downstream signaling. *Int Immunopharmacol* **103**,  
924 108456 (2021).
- 925 35. S. C. Cheng *et al.*, Broad defects in the energy metabolism of leukocytes underlie immunoparalysis in  
926 sepsis. *Nat Immunol* **17**, 406-413 (2016).
- 927 36. C. Nedeva, J. Menassa, H. Puthalakath, Sepsis: Inflammation Is a Necessary Evil. *Front Cell Dev Biol*  
928 **7**, 108 (2019).
- 929 37. C. A. Gogos, E. Drosou, H. P. Bassaris, A. Skoutelis, Pro- versus anti-inflammatory cytokine profile in  
930 patients with severe sepsis: a marker for prognosis and future therapeutic options. *J Infect Dis* **181**,  
931 176-180 (2000).
- 932 38. J. T. van Dissel, P. van Langevelde, R. G. Westendorp, K. Kwappenberg, M. Frölich, Anti-inflammatory  
933 cytokine profile and mortality in febrile patients. *Lancet* **351**, 950-953 (1998).
- 934 39. M. De Zuani, J. Frič, Train the Trainer: Hematopoietic Stem Cell Control of Trained Immunity. *Front*  
935 *Immunol* **13**, 827250 (2022).
- 936 40. S. E. Vasquez, M. A. Inlay, T. Serwold, CD201 and CD27 identify hematopoietic stem and progenitor  
937 cells across multiple murine strains independently of Kit and Sca-1. *Experimental Hematology*, (2015).
- 938 41. B. Nowlan, E. D. Williams, M. R. Doran, J.-P. Levesque, CD27, CD201, FLT3, CD48, and CD150 cell  
939 surface staining identifies long-term mouse hematopoietic stem cells in immunodeficient non-obese  
940 diabetic severe combined immune deficient-derived strains. *Haematologica*, (2020).
- 941 42. R. M. Dougherty, C. Galli, A. Ferro-Luzzi, J. M. Iacono, Lipid and phospholipid fatty acid composition of  
942 plasma, red blood cells, and platelets and how they are affected by dietary lipids: a study of normal  
943 subjects from Italy, Finland, and the USA. *Am J Clin Nutr* **45**, 443-455 (1987).
- 944 43. C. M. Skeaff, L. Hodson, J. E. McKenzie, Dietary-induced changes in fatty acid composition of human  
945 plasma, platelet, and erythrocyte lipids follow a similar time course. *J Nutr* **136**, 565-569 (2006).

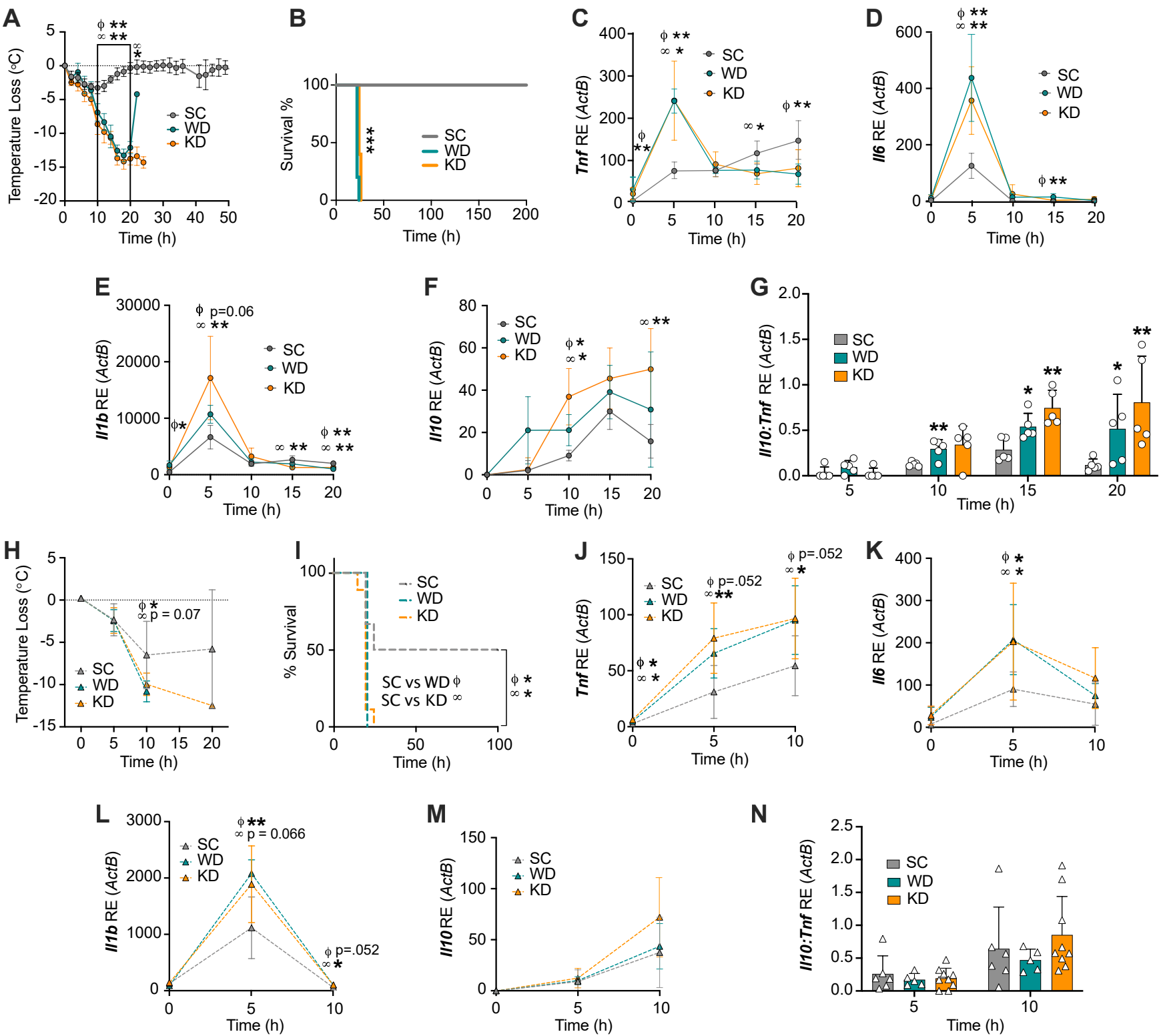
- 946 44. N. Zollner, F. Tato, Fatty acid composition of the diet: impact on serum lipids and atherosclerosis. *Clin*  
947 *Investig* **70**, 968-1009 (1992).
- 948 45. J. Choi *et al.*, Comprehensive analysis of phospholipids in the brain, heart, kidney, and liver: brain  
949 phospholipids are least enriched with polyunsaturated fatty acids. *Mol Cell Biochem* **442**, 187-201  
950 (2018).
- 951 46. I. S. S. A, A. B. C, J. S. A, Changes in Plasma Free Fatty Acids Associated with Type-2 Diabetes.  
952 *Nutrients* **11**, (2019).
- 953 47. E. Sokolowska, A. Blachnio-Zabielska, The Role of Ceramides in Insulin Resistance. *Front Endocrinol*  
954 *(Lausanne)* **10**, 577 (2019).
- 955 48. M. Papadimitriou-Olivgeris *et al.*, The Role of Obesity in Sepsis Outcome among Critically Ill Patients: A  
956 Retrospective Cohort Analysis. *Biomed Res Int* **2016**, 5941279 (2016).
- 957 49. A. Mancini *et al.*, Biological and Nutritional Properties of Palm Oil and Palmitic Acid: Effects on Health.  
958 *Molecules* **20**, 17339-17361 (2015).
- 959 50. J. Korbecki, K. Bajdak-Rusinek, The effect of palmitic acid on inflammatory response in macrophages:  
960 an overview of molecular mechanisms. *Inflamm Res* **68**, 915-932 (2019).
- 961 51. S. A. Abdelmagid *et al.*, Comprehensive Profiling of Plasma Fatty Acid Concentrations in Young  
962 Healthy Canadian Adults. *PLoS One*, (2015).
- 963 52. L. Liu *et al.*, Targeted metabolomic analysis reveals the association between the postprandial change in  
964 palmitic acid, branched-chain amino acids and insulin resistance in young obese subjects. *Diabetes*  
965 *Res Clin Pract* **108**, 84-93 (2015).
- 966 53. S. F. Gallego, M. Hermansson, G. Liebisch, L. Hodson, C. S. Ejsing, Total Fatty Acid Analysis of  
967 Human Blood Samples in One Minute by High-Resolution Mass Spectrometry. *Biomolecules* **9**, (2018).
- 968 54. C. D. C. Buchanan *et al.*, Analysis of major fatty acids from matched plasma and serum samples  
969 reveals highly comparable absolute and relative levels. *Prostaglandins, Leukotrienes and Essential*  
970 *Fatty Acids* **168**, 102268 (2021).
- 971 55. M. Perreault *et al.*, A distinct fatty acid profile underlies the reduced inflammatory state of metabolically  
972 healthy obese individuals. *PLoS One* **9**, e88539 (2014).

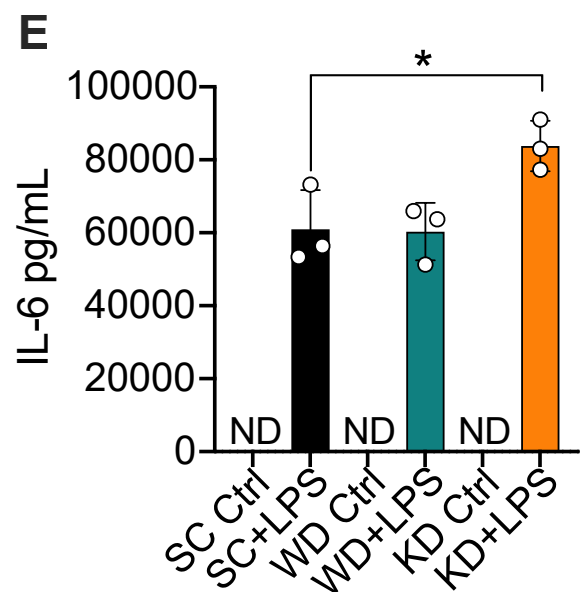
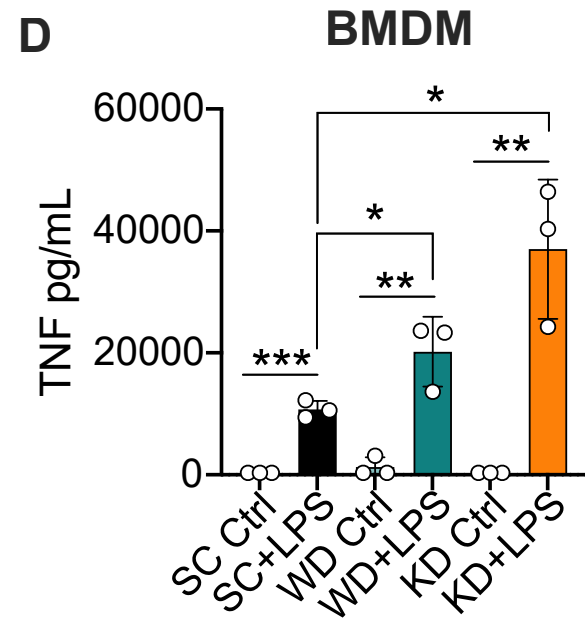
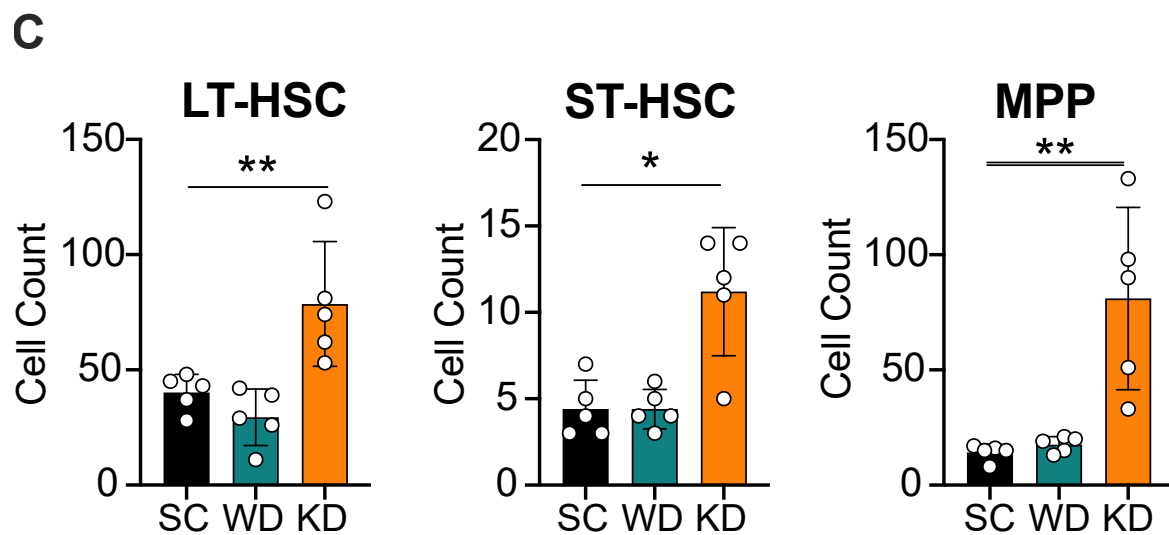
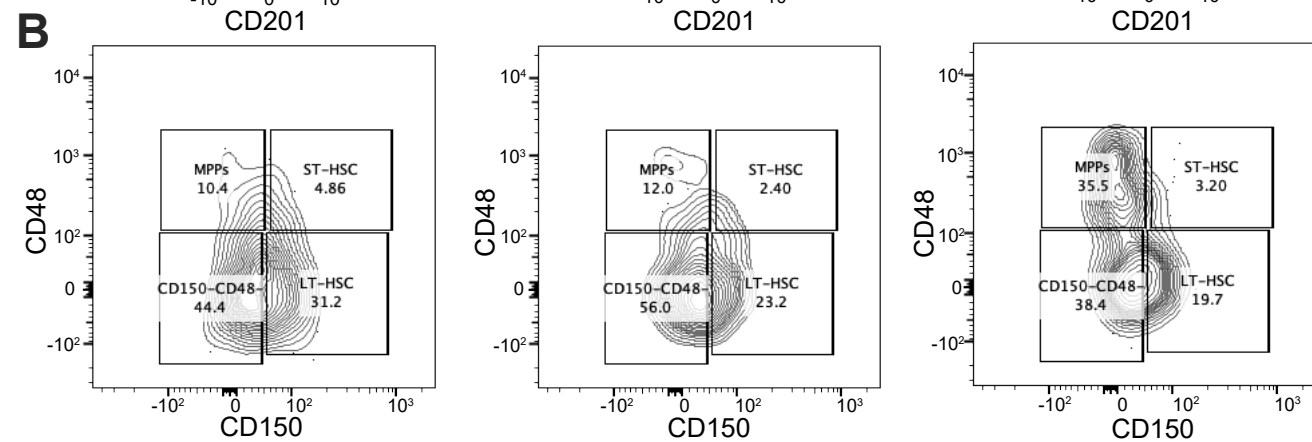
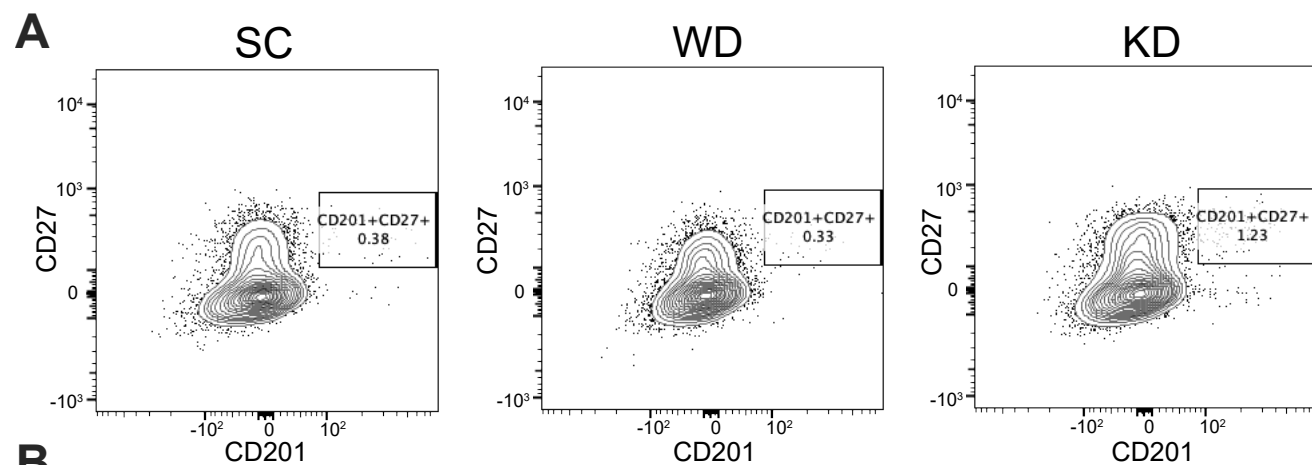
- 973 56. N. M. Borradaile *et al.*, Disruption of endoplasmic reticulum structure and integrity in lipotoxic cell death.  
974 *J Lipid Res* **47**, 2726-2737 (2006).
- 975 57. H. Li *et al.*, Adipocyte Fatty Acid-Binding Protein Promotes Palmitate-Induced Mitochondrial  
976 Dysfunction and Apoptosis in Macrophages. *Front Immunol* **9**, 81 (2018).
- 977 58. L. D. Ly *et al.*, Oxidative stress and calcium dysregulation by palmitate in type 2 diabetes. *Exp Mol Med*  
978 **49**, e291 (2017).
- 979 59. L. Tao *et al.*, RIP1 kinase activity promotes steatohepatitis through mediating cell death and  
980 inflammation in macrophages. *Cell Death Differ* **28**, 1418-1433 (2021).
- 981 60. X. Palomer, J. Pizarro-Delgado, E. Barroso, M. Vázquez-Carrera, Palmitic and Oleic Acid: The Yin and  
982 Yang of Fatty Acids in Type 2 Diabetes Mellitus. *Trends in Endocrinology & Metabolism* **29**, 178-190  
983 (2018).
- 984 61. J. Jin *et al.*, Acid sphingomyelinase plays a key role in palmitic acid-amplified inflammatory signaling  
985 triggered by lipopolysaccharide at low concentrations in macrophages. *Am J Physiol Endocrinol Metab*  
986 **305**, E853-867 (2013).
- 987 62. K. Eguchi *et al.*, Saturated fatty acid and TLR signaling link beta cell dysfunction and islet inflammation.  
988 *Cell Metab* **15**, 518-533 (2012).
- 989 63. D. D. Black, Development and Physiological Regulation of Intestinal Lipid Absorption. I. Development of  
990 intestinal lipid absorption: cellular events in chylomicron assembly and secretion. *Am J Physiol*  
991 *Gastrointest Liver Physiol* **293**, (2007).
- 992 64. C. M. Mansbach II, F. Gorelick, Development and physiological regulation of intestinal lipid absorption.  
993 II. Dietary lipid absorption, complex lipid synthesis, and the intracellular packaging and secretion of  
994 chylomicrons. *Am J Physiol Gastrointest Liver Physiol* **293**, (2007).
- 995 65. M. H. Karavolos *et al.*, Adrenaline modulates the global transcriptional profile of Salmonella revealing a  
996 role in the antimicrobial peptide and oxidative stress resistance responses. *BMC Genomics* **9**, 458  
997 (2008).
- 998 66. M. G. Netea *et al.*, Defining trained immunity and its role in health and disease. *Nat Rev Immunol* **20**,  
999 375-388 (2020).

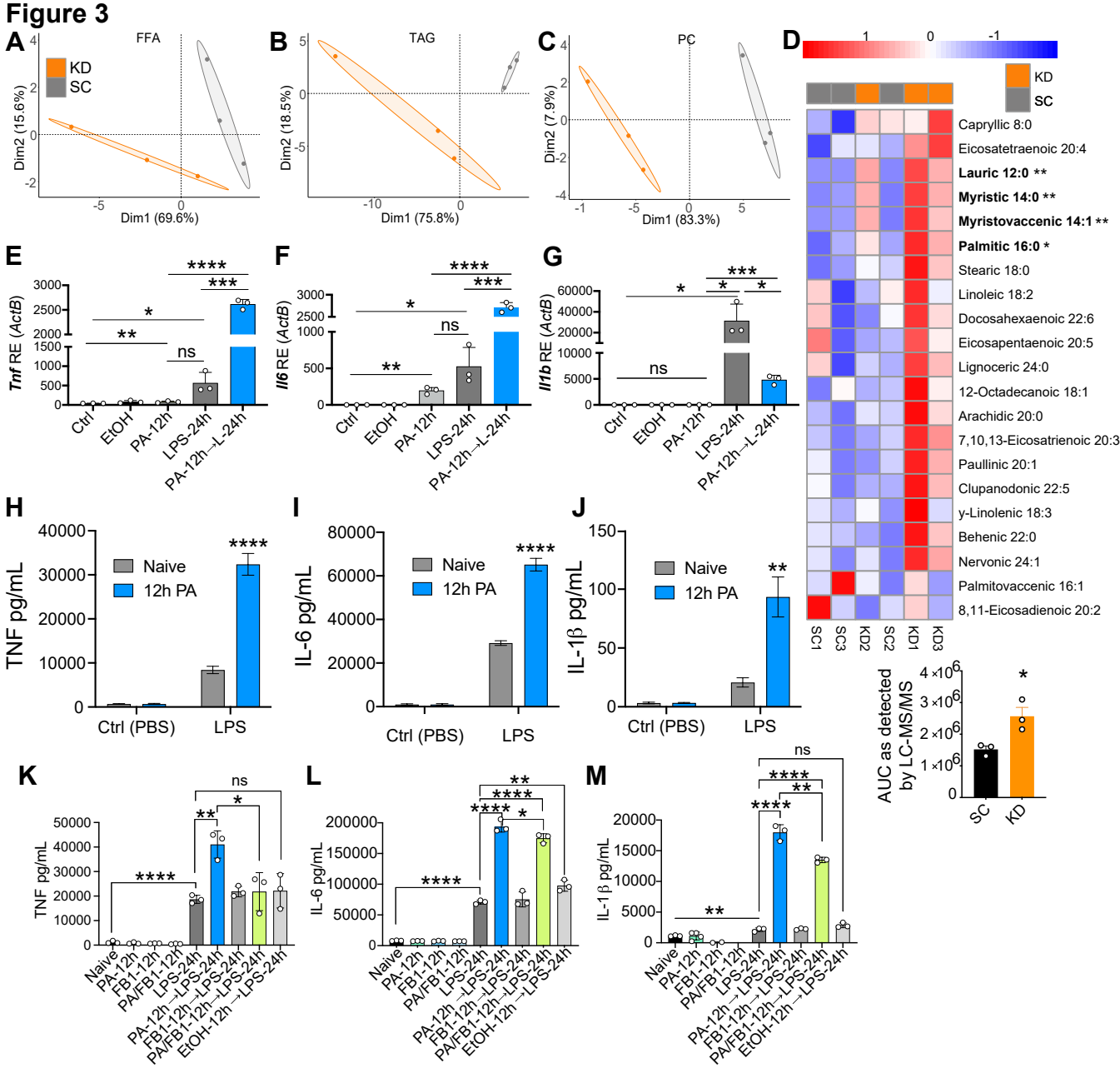
- 000 67. L. L. Listenberger *et al.*, Triglyceride accumulation protects against fatty acid-induced lipotoxicity. *Proc*  
001 *Natl Acad Sci U S A* **100**, 3077-3082 (2003).
- 002 68. S. Bekkering *et al.*, Oxidized low-density lipoprotein induces long-term proinflammatory cytokine  
003 production and foam cell formation via epigenetic reprogramming of monocytes. *Arterioscler Thromb*  
004 *Vasc Biol* **34**, 1731-1738 (2014).
- 005 69. T. S. Ayala *et al.*, High glucose environments interfere with bone marrow-derived macrophage  
006 inflammatory mediator release, the TLR4 pathway and glucose metabolism. *Scientific Reports*, (2019).
- 007 70. P. Y. Ng, M. Eikermann, The obesity conundrum in sepsis. *BMC Anesthesiol* **17**, 147 (2017).
- 008 71. K. D. Hall, S. T. Chung, Effect of a plant-based, low-fat diet versus an animal-based, ketogenic diet on  
009 ad libitum energy intake. *Nature Medicine*, (2021).
- 010 72. A. R. Kennedy, E. Maratos-Flier, A high-fat, ketogenic diet induces a unique metabolic state in mice.  
011 *The American Journal of Physiology - Endocrinology and Metabolism*, (2007).
- 012 73. S. Galadari, A. Rahman, S. Pallichankandy, A. Galadari, F. Thayyullathil, Role of ceramide in diabetes  
013 mellitus: evidence and mechanisms. *Lipids Health Dis* **12**, 98 (2013).
- 014 74. A. R. DiNardo, M. G. Netea, D. M. Musher, Postinfectious Epigenetic Immune Modifications - A Double-  
015 Edged Sword. *N Engl J Med* **384**, 261-270 (2021).
- 016 75. B. Beutler, I. W. Milsark, A. C. Cerami, Passive immunization against cachectin/tumor necrosis factor  
017 protects mice from lethal effect of endotoxin. *Science* **229**, 869-871 (1985).
- 018 76. K. M. Mohler *et al.*, Soluble tumor necrosis factor (TNF) receptors are effective therapeutic agents in  
019 lethal endotoxemia and function simultaneously as both TNF carriers and TNF antagonists. *J Immunol*  
020 **151**, 1548-1561 (1993).
- 021 77. P. N. Cunningham *et al.*, Acute renal failure in endotoxemia is caused by TNF acting directly on TNF  
022 receptor-1 in kidney. *J Immunol* **168**, 5817-5823 (2002).
- 023 78. Y. Chen *et al.*, Aerosol synthesis of cargo-filled graphene nanosacks. *Nano Lett* **12**, 1996-2002 (2012).
- 024 79. W. Zhong *et al.*, Curcumin alleviates lipopolysaccharide induced sepsis and liver failure by suppression  
025 of oxidative stress-related inflammation via PI3K/AKT and NF- $\kappa$ B related signaling. *Biomed*  
026 *Pharmacother* **83**, 302-313 (2016).

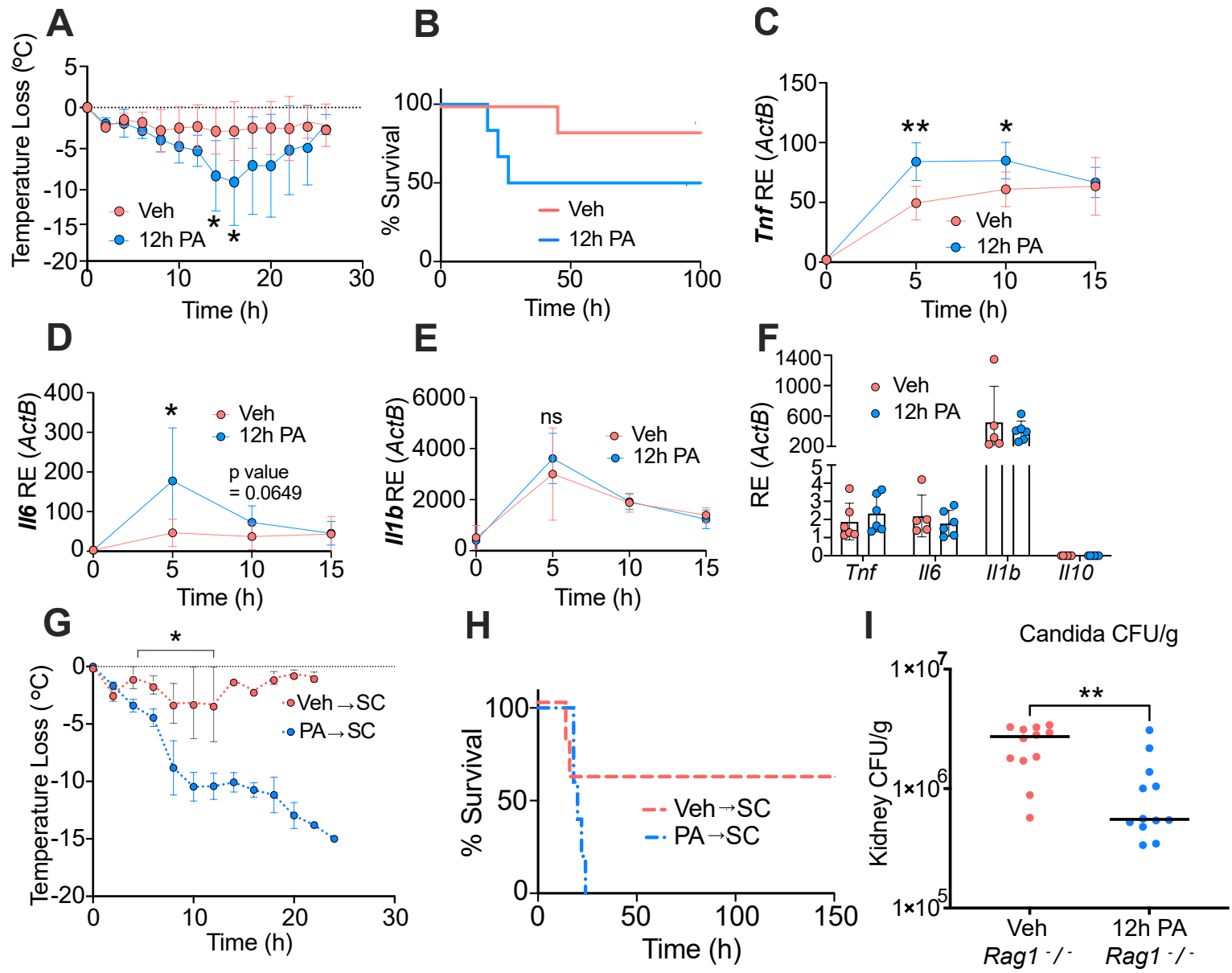
- 027 80. L. E. Escobar, A. Molina-Cruz, C. Barillas-Mury, BCG vaccine protection from severe coronavirus  
028 disease 2019 (COVID-19). *Proc Natl Acad Sci U S A* **117**, 17720-17726 (2020).
- 029 81. R. J. Arts *et al.*, Glutaminolysis and Fumarate Accumulation Integrate Immunometabolic and Epigenetic  
030 Programs in Trained Immunity. *Cell Metab* **24**, 807-819 (2016).
- 031 82. D. G. Ryan, L. A. J. O'Neill, Krebs Cycle Reborn in Macrophage Immunometabolism. *Annu Rev*  
032 *Immunol* **38**, 289-313 (2020).
- 033 83. G. D. Silva, F. C. Brochers-Lacchini, A. M. Leopoldino, How do sphingolipids play a role in epigenetic  
034 mechanisms and gene expression? *Epigenomics*, (2021).
- 035 84. D. G. Souza *et al.*, The essential role of the intestinal microbiota in facilitating acute inflammatory  
036 responses. *J Immunol* **173**, 4137-4146 (2004).
- 037 85. A. K. F. Mundt *et al.* (2017).
- 038 86. Wickham *et al.* (Springer International Publishing, 2016).
- 039 87. Lê *et al.*, FactoMineR: an R package for multivariate analysis. *J. Stat. Soft* (2008).
- 040 88. Kolde *et al.* (2018).
- 041

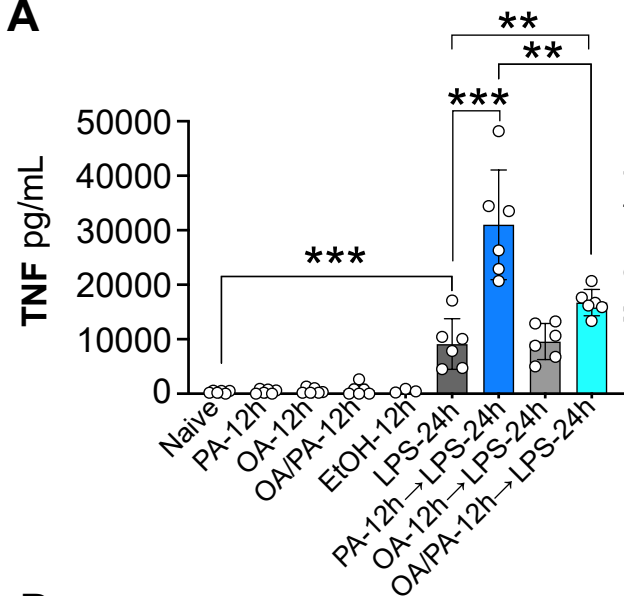
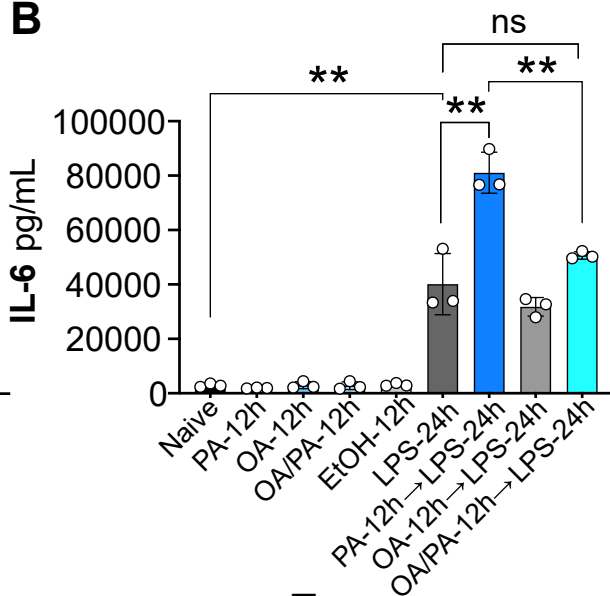
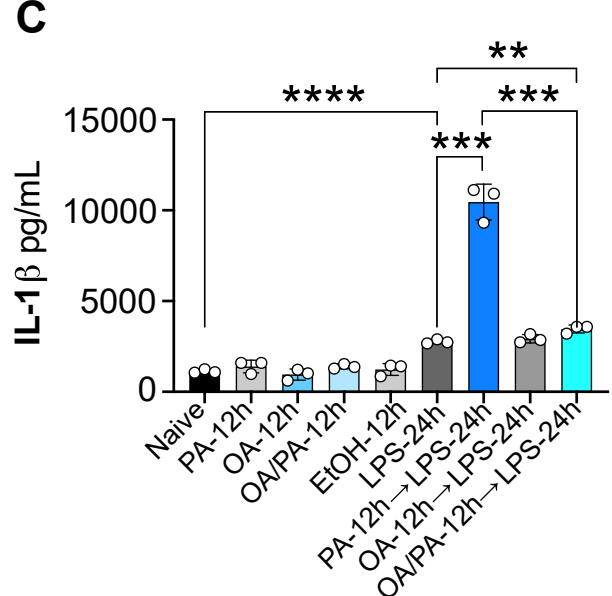
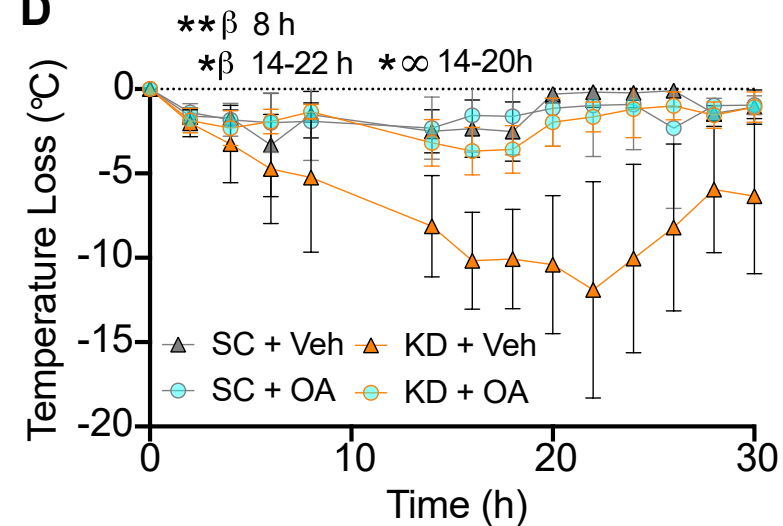
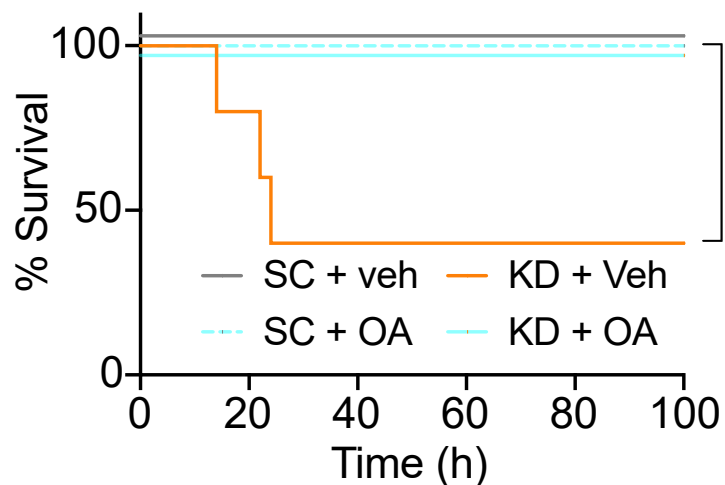


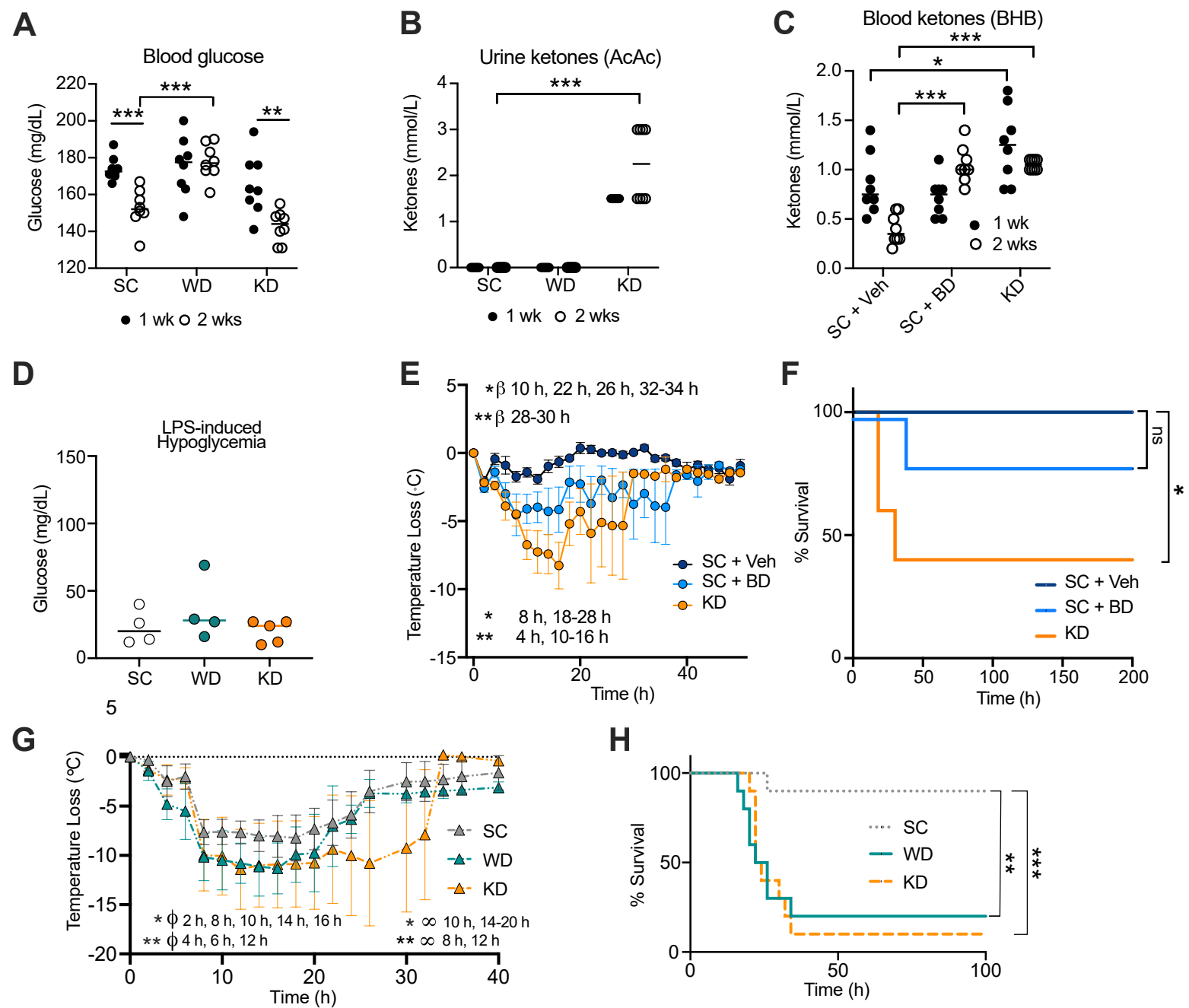
**Figure 1**

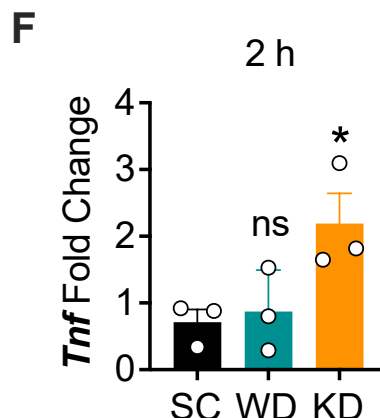
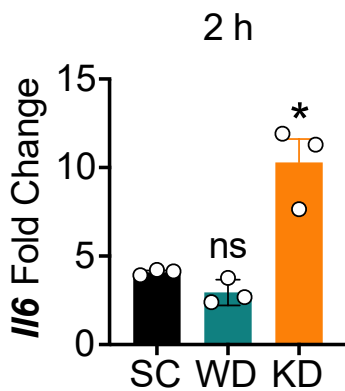
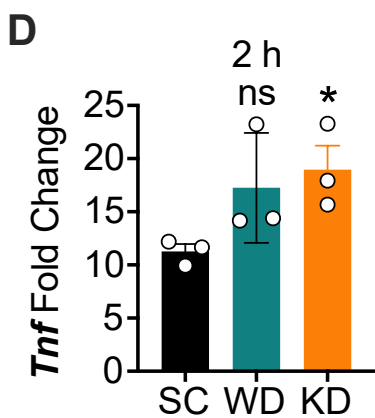
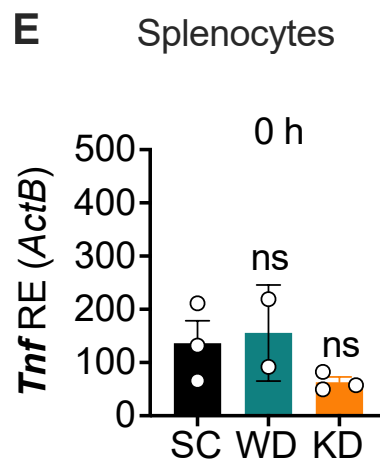
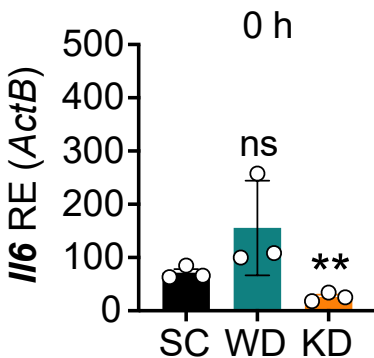
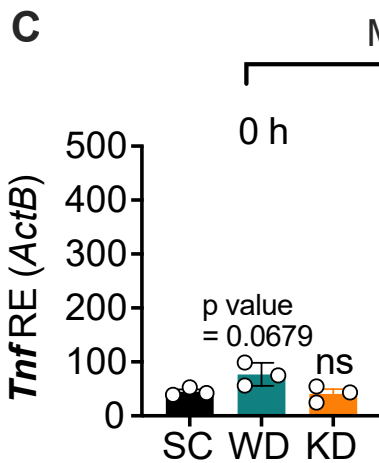
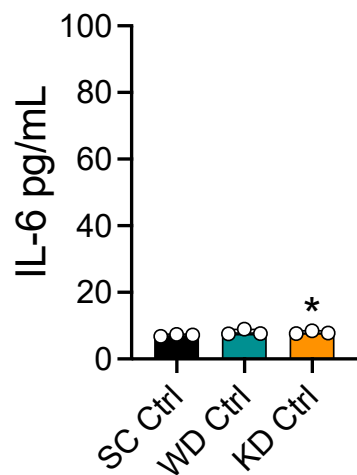
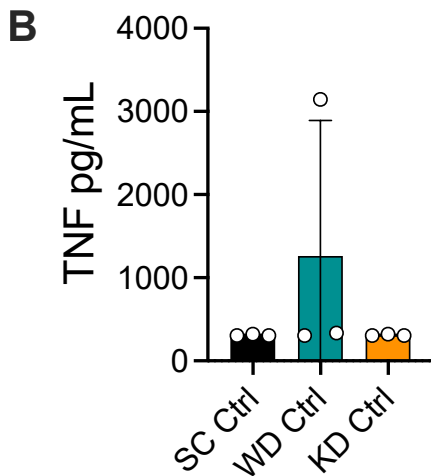
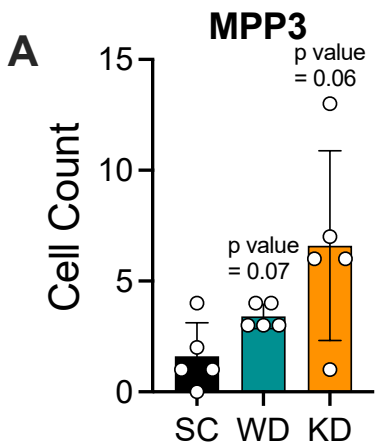
**Figure 2**

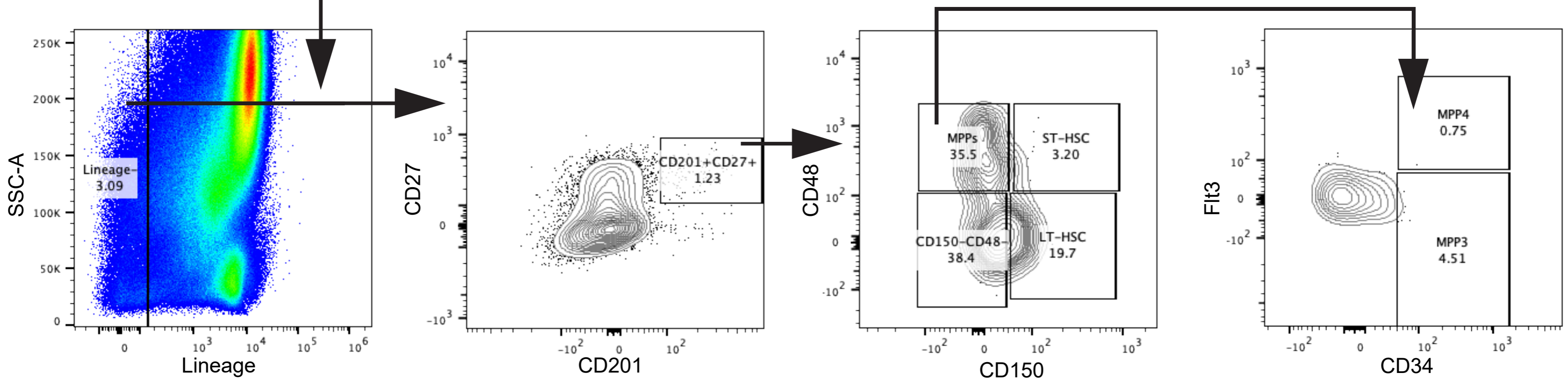
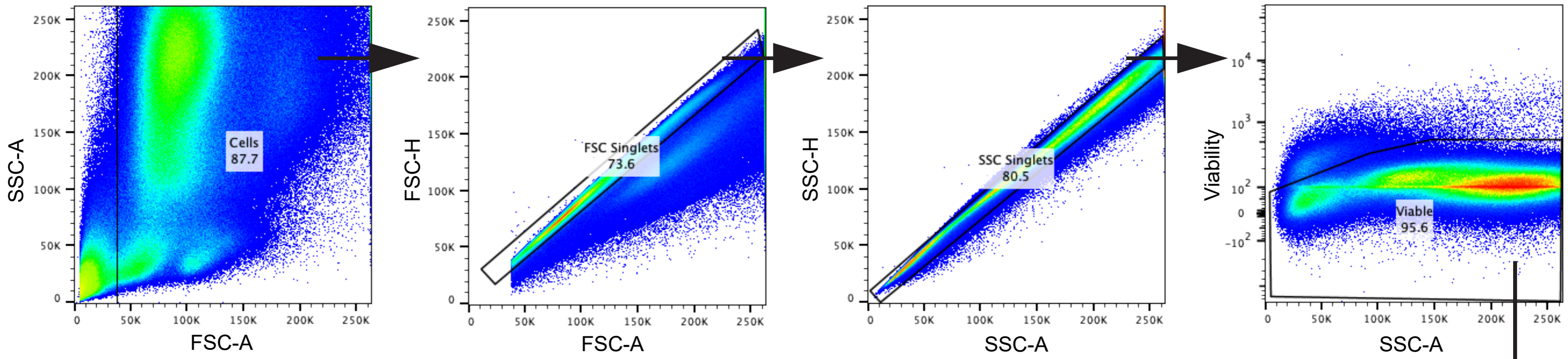


**Figure 4**

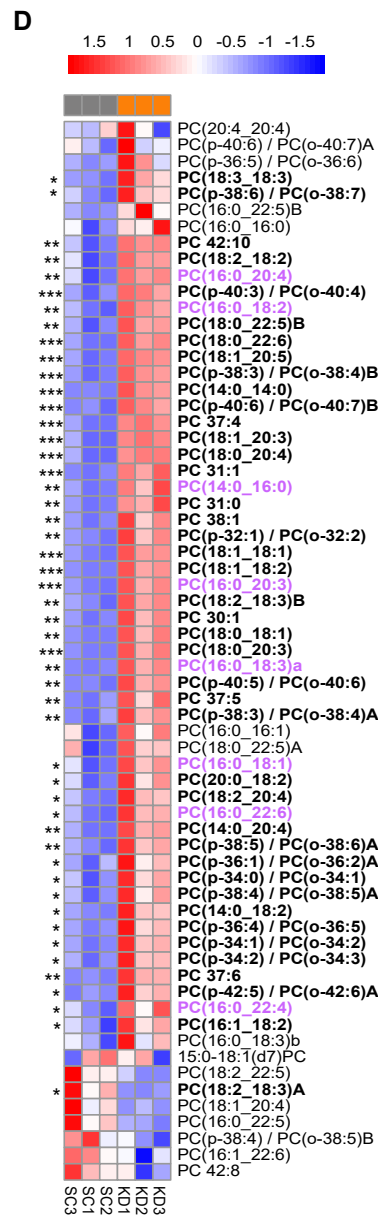
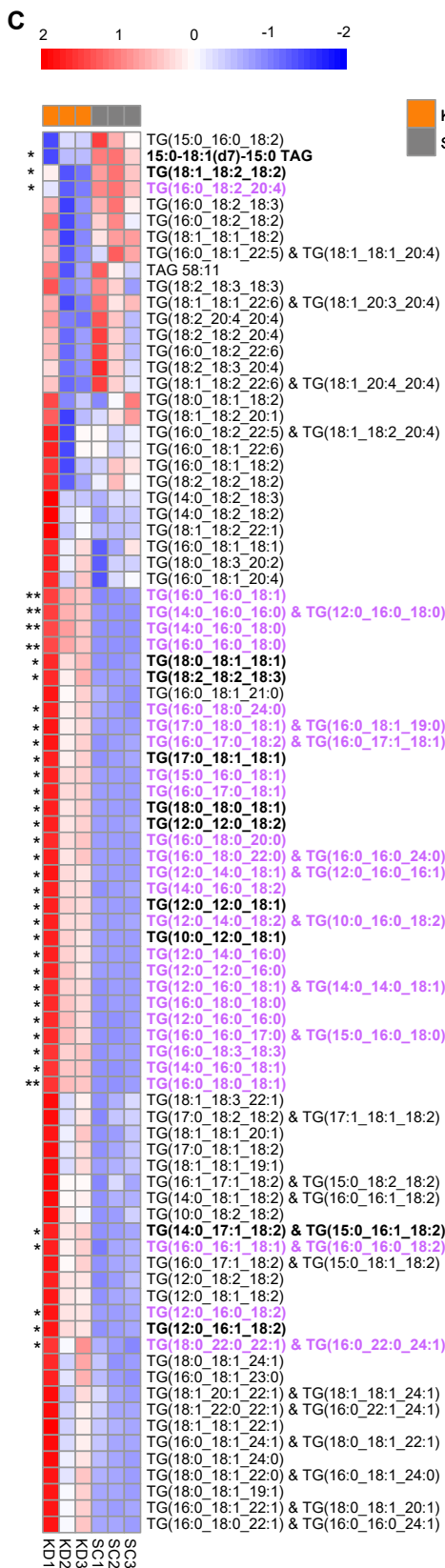
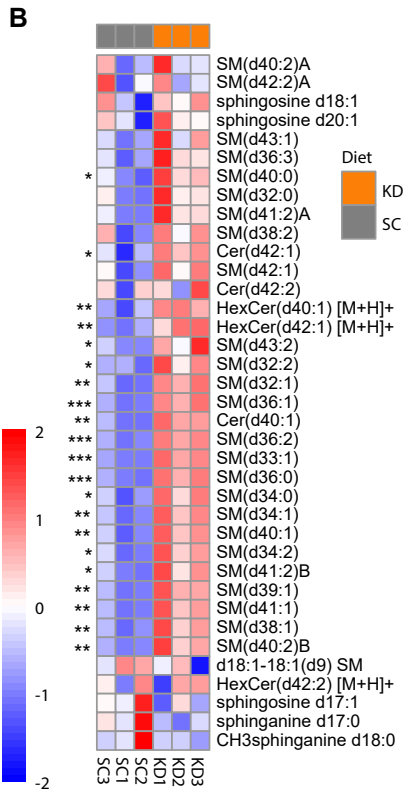
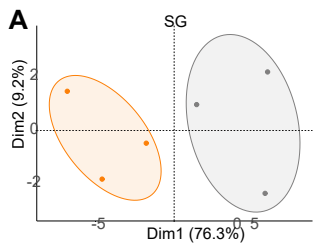
**Figure 5****A****B****C****D****E**

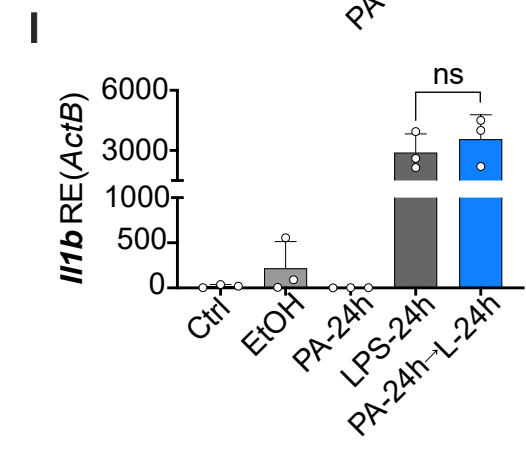
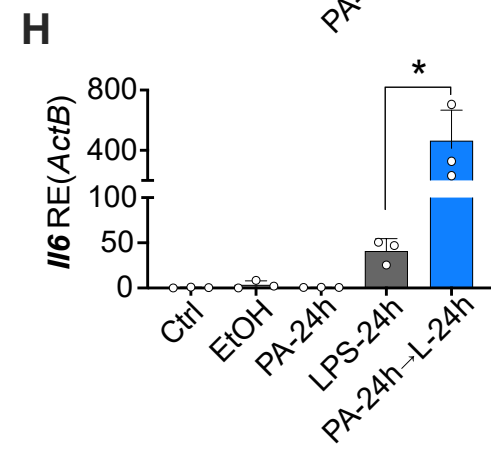
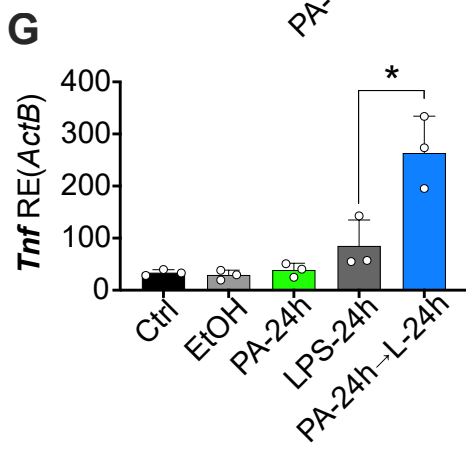
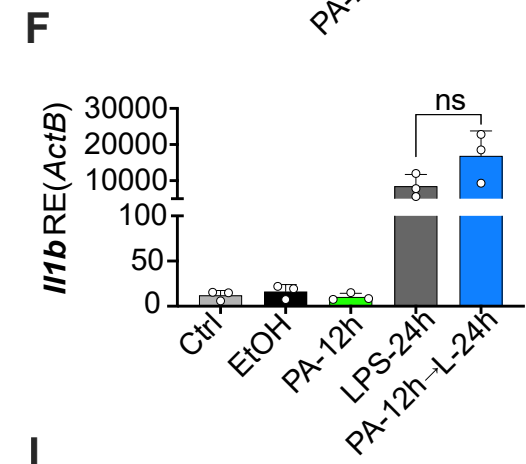
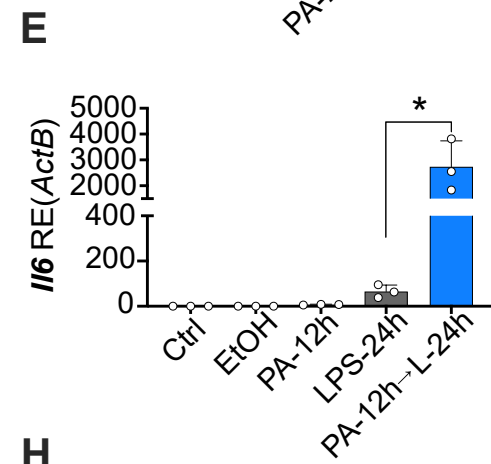
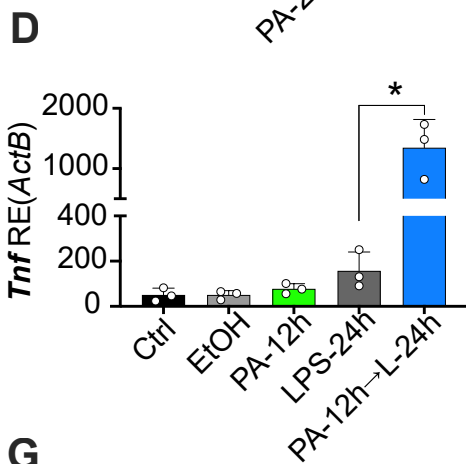
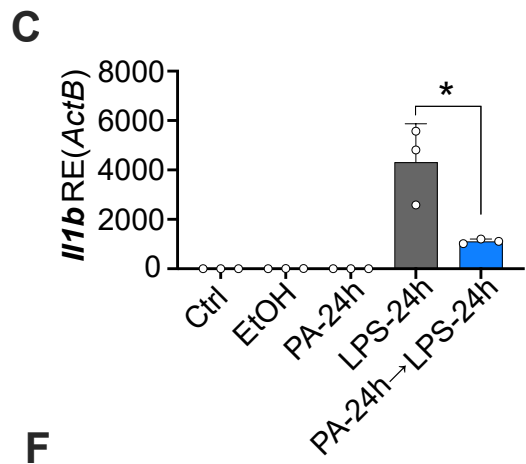
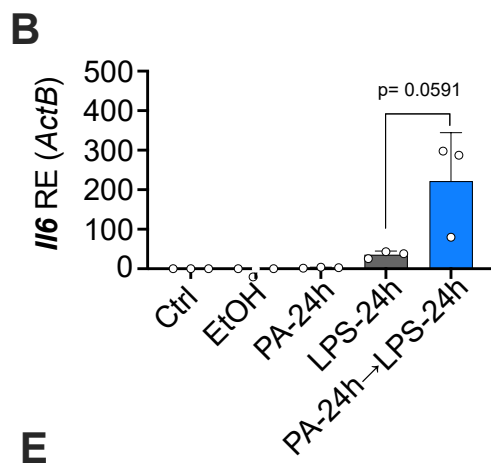
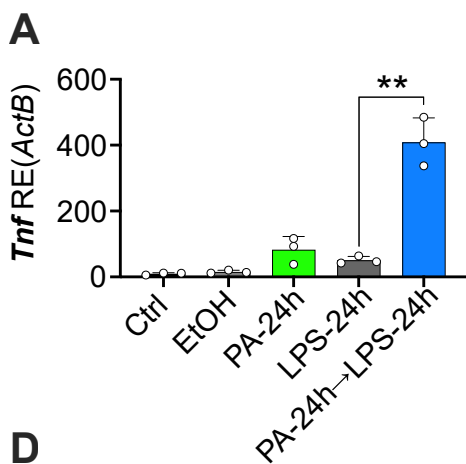




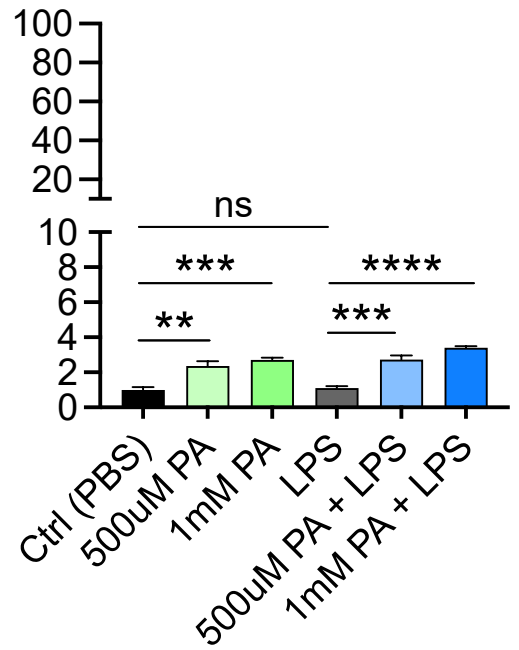




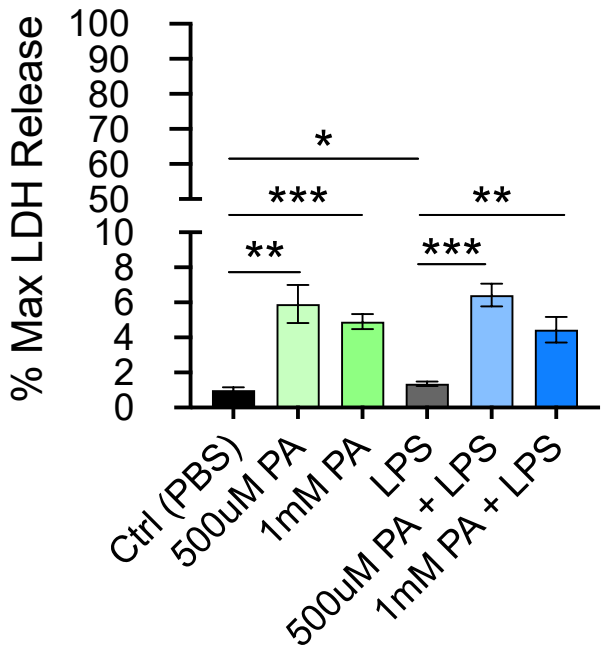


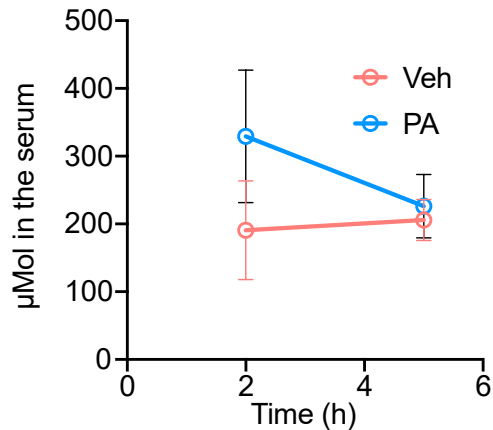
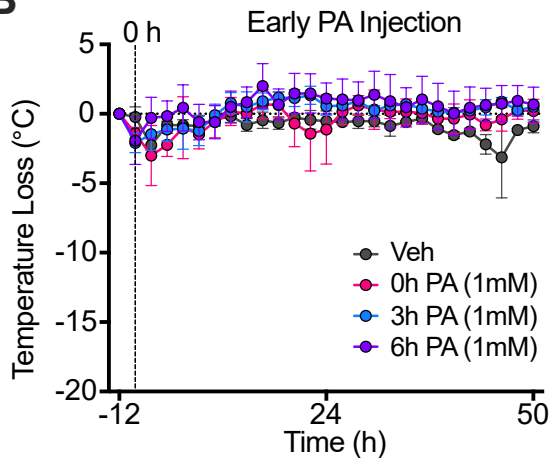
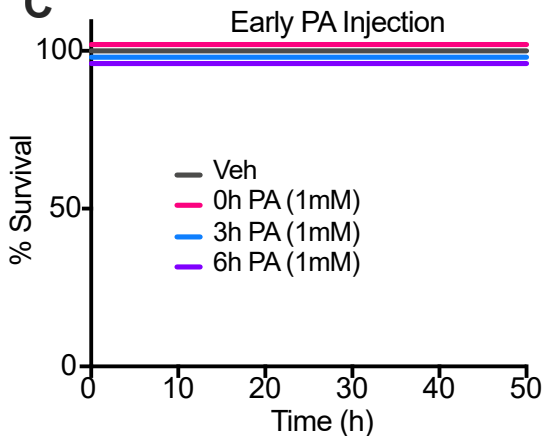


# A



# B



**A****B****C****D**